New two-phase multiplier model for phase-change flows in plate heat exchangers

Yagnavalkya Mukkamala[a*], Jaco Dirker[b]

[a]School of Mechanical Engineering, Vellore Institute of Technology, Vellore, India

[b]Department of Mechanical and Aeronautical Engineering, University of Pretoria, South Africa

ABSTRACT

A complete thermo-hydraulic understanding of condensing and evaporating flows in heat exchangers requires predictive modeling and analysis of not just heat transfer but also the hydraulics of the flow. While modeling the friction factor and pressure gradient yields a quantitative understanding of the pressure drop, only the two-phase multiplier and void fraction, in combination with the Martinelli parameter, help better understand the relative contributions of the liquid and vapor fractions to the overall pressure drop. This article reports the empirical modeling, analysis, and meta-analysis of the two-phase multiplier for condensing and evaporating flows in plate heat exchangers. Over three thousand data compiled from forty-two sources were modeled using various regression techniques to develop correlations for predicting the two-phase multiplier for condensing and evaporating flows in plate heat exchangers. The Weber number for most studies was less than one, indicating that drop condensation and pool boiling were impossible. Further, the Bond number for most studies was also much higher than one, indicating that the buoyancy effects were significant during condensation and evaporation. Meta-analysis for evaporators was statistically significant and positive, strongly recommending plate heat exchangers. The predictive condensation two-phase multiplier correlation is valid for the liquid-only Reynolds number Re_{LO} = 13-7105, vapor quality $0 < x < 1$, saturation pressure P_{sat} = 0.9-24.26 bar, heat flux q" = 0-20 kW/m^2,

mass flux G = 2.5-150 kg/m^{2}s, hydraulic diameter d_h = 2.99-6.6 mm and chevron angle β = 30-65°. Similarly, the evaporation two-phase multiplier correlation is valid for the liquid-only Reynolds number Re_{LO} = 19-4870, saturation pressure P_{sat} = 0.165-27.63 bar, heat flux q" = 0-49.1 kW/m^2, mass flux G = 5.5-140 kg/m^{2}s, vapor quality 0 < x < 1, hydraulic diameter d_h = 1.7-15 mm, chevron angle β = 20-65°, and reduced pressure P_r = 0.005-0.65.

∗Corresponding Author. Address: School of Mechanical Engineering, Vellore Institute of Technology, Vellore 632014, India; Phone 91-9345310732; 91-0416-2202203; e-mail: yagnasmukkamala@vit.ac.in; Fax: 91-416-2243092

Introduction

Plate heat exchangers (PHEs) are frequently used in the process industry for heat exchange between hot and cold fluids. Since they are more compact than conventional shell-and-tube heat exchangers (HX), PHEs offer a viable alternative to space-constrained industries and allow quick and easy retrofitting. Unlike conventional HXs, PHEs also increase the aspect ratio or the surface area of the HX per unit volume, thereby enhancing the heat transfer rate. In a recent article [1], the authors modeled the friction pressure drop in plate heat exchangers and developed correlations for predicting the two-phase friction factor in PHE-based condensers and evaporators. Although friction factors can be used to model and estimate the total pressure drop and pump duty in PHE condensers and evaporators, they don't assess the relative contributions of the liquid and vapor phases to the overall pressure drop. The wetted perimeters of the liquid and vapor fractions indicate the nature of the local flow in PHEs and the attendant pressure drop. Just as the individual hydraulic diameters of the liquid and vapor fractions are less than the pipe diameter, the particular pressure drop contributions of the liquid and vapor phases will be less than the total two-phase pressure drop. To estimate these relative contributions of the liquid and vapor fractions to the total pressure drop, this article will develop

a new correlation for the liquid-only two-phase multiplier ϕ_{LO}. The two-phase multiplier is defined as:

$$\phi_{LO}^2 = \frac{\left(\frac{dP}{dZ}\right)_{TP}}{\left(\frac{dP}{dZ}\right)_{LO}} \quad (1)$$

It estimates the contribution of the liquid-only flow-induced pressure drop compared to the two-phase pressure drop resulting from the combined liquid and vapor flows. Along with the Martinelli parameter X, which estimates the ratio of the vapor and liquid phase pressure gradients, the two-phase multiplier ϕ_{LO} will assess the relative contributions of the liquid and vapor phases to the total two-phase pressure drop in PHE condensers and evaporators. Since the Martinelli parameter involves the relative weight fractions of the liquid and vapor flows, a combination of the two-phase multiplier ϕ_{LO} and the Martinelli parameter X would also estimate the wetted perimeters and hydraulic diameters of the liquid and vapor fractions in two-phase flows. This article intends to improve the understanding of the underlying mechanisms during two-phase pressure drop in PHE condensers and evaporators by estimating the individual contributions of the liquid and vapor phases to the total two-phase pressure drop.

Developing reliable and precise predictive correlations is necessary for successfully designing PHE condensers and evaporators. The accuracy of the predictive correlation is related to the complexity of the correlation. Further, the choice of the flow modifiers in the correlation should be flow regime-dependent to reflect the regional flow physics accurately. To achieve this objective, this article has compiled condensation pressure drop data in PHE condensers from seventeen sources [2-18], which was assessed with widely cited research [19-22] and evaluated with independent data [15, 23-24]. Similarly, evaporation pressure drop data was compiled from twenty-four sources [25-48] and assessed with published research [33, 49-51] while being evaluated with independent data [52]. Only a few phase-change two-phase multiplier ϕ_{LO} predictive correlations [12, 19-22, 49 and 51] in PHEs are currently available,

while the rest are only for two-phase flows [33-34, 50] without phase-change. The phase-change process-based two-phase multiplier correlations are based on the liquid Reynolds number Re_L and the Martinelli parameter X. While they may accurately model the wetted perimeters and liquid and vapor fractions, they fail to estimate the buoyancy, surface tension, and slip effects. The correlations without any phase change are merely the modifications of the Lockhart and Martinelli constant C [50] and are not accurate for condensing and evaporating flows in PHEs. Consequently, this article also intends to improve the existing models for predicting the two-phase multiplier and phase-change pressure drop in PHE condensers and evaporators. It incorporates the buoyancy, slip, and surface tension effects during phase-change pressure drop in terms of the Bond number Bd, Convection number Co, and Weber number We, respectively. The wetted perimeter of the liquid and vapor fractions will be modeled accurately using the Martinelli parameter X.

Given the volume of existing data currently available, the authors felt it was necessary to assess the reliability of the current data before producing more. A meta-analysis was conducted to evaluate the existing data's reliability and dependability. The compiled data was reduced to standard normalized parameters such as the liquid-only Reynolds number Re_{LO}, Convection number Co, Martinelli parameter X, etc., so that the diverse data would have similitude and could be compared. Meta-analysis revealed considerable heterogeneity and inconsistency in the available data, indicating that on a normalized basis, different tests investigating the same problem at the same liquid-only Reynolds number Re_{LO} and control parameters yielded widely different two-phase multiplier ϕ_{LO} values when they should have been similar. This issue will be addressed further in subsequent sections.

To summarize, this article aims to improve the understanding of the phase-change flow physics in PHE condensers and evaporators by better modeling the wetted perimeters of the liquid and vapor fractions and their relative contributions to the two-phase pressure drop in

PHEs. Compared to existing works, the significance of this article is that, unlike existing correlations, this research developed more complex predictive correlations for estimating the two-phase multipliers and liquid and vapor fraction contributions to the pressure drop by incorporating the buoyancy, slip, and surface tension effects. While the current correlations are based on limited data, the presented correlations are more universal and comprehensive based on all the available data from the past three decades. Compared to any other work, the novelty of this article is that it performed a meta-analysis of existing data to assess the reliability, consistency, and dependability of the current phase-change two-phase multipliers computed from data. Such an analysis is unique and currently unavailable in the literature. The study strongly suggests that PHE evaporators are highly recommended as phase-change HXs in the process industry and preferable to the existing shell-and-tube and other configurations.

The authors believe the sophisticated empirical models, analysis, and insights would benefit the practicing engineer in the industry and academia.

Sources and filtering

The database and the criteria for filtering the sources are discussed in this section. Ten databases that included the Web of Science, Springer, Google Scholar, Taylor and Francis, ASME digital collection, ScienceDirect, SAE Mobilus, ProQuest, EBSCO, and SAGE Journals were searched with keywords to discover over two hundred thousand records. These were then filtered using the following criteria:

a. Criteria for selection:
    i) Articles must be full-length and published in peer-reviewed journals or conference proceedings.
    ii) Articles must be focused on phase change (evaporation or condensation) and not just two-phase (ex: air-water flow) flows.

iii) Articles must either have experimental pressure drop ΔP or the pressure gradient dP/dZ in PHE condensers or evaporators. Other types of heat exchangers were discarded.

iv) Articles must provide local or surface-averaged data that varied with the vapor quality x.

b. Criteria for exclusion:

i) Abstracts, short-length papers, and those without full access were discarded. Articles published in predatory journals and not listed in the Web of Science were discarded.

ii) Experiments in other heat exchangers were discarded.

iii) Experiments without phase-change data (ex, air-liquid flow without phase-change) were discarded.

iv) Experiments without the spatial variation of the pressure drop ΔP or the pressure gradient dP/dZ with the vapor quality x were discarded (ex: ΔP or dP/dZ vs. the mass flux G without the vapor quality x were excluded)

v) Articles without numerical uncertainty limits or at least a discussion of experimental uncertainty were discarded.

Forty-one investigations in PHEs, seventeen condensation studies, and twenty-four evaporation studies were short-listed for data compilation, modeling, analysis, and critique. Figures 1-2 depict the database and records search.

Condensers

One thousand four hundred and twenty-eight data were collected from seventeen experimental investigations in PHE condensers. Table 1 lists all the studies discussed in this section. Table 2 gives a comparative analysis of the database.

Yan et al. [2] investigated the condensation of R134a in a 6.6 mm hydraulic diameter and a sixty-degree chevron angle PHE condenser. The saturation pressure P_{sat} was constant at 7 bar while the heat flux q" was constant at 10 kW/m^2. The vapor quality x went from 0.1 to 0.9, while the mass flux G ran from 60 kg/m^{2}s to 120 kg/m^{2}s. A new two-phase friction factor f_{TP} correlation was proposed, but no correlation was developed for the two-phase multiplier ϕ_{LO}.

Kuo et al. [3] conducted condensation pressure drop experiments with R410A in a 6.6 mm hydraulic diameter and a sixty-degree chevron angle PHE condenser. The saturation pressure P_{sat} varied between 14.4 and 19.5 bar while the heat flux q" went from 10 kW/m^2 to 20 kW/m^2. The vapor quality x ranged from 0.1 to 0.9, while the mass flux G ran from 50 kg/m^{2}s to 150 kg/m^{2}s. The two-phase friction factor f_{TP} dropped by 60% as the vapor quality x increased from 0.02 to 0.82. No new correlations were reported for the two-phase multiplier ϕ_{LO}.

Djordjevic et al. [4] reported condensation pressure drop data in a 3.2 mm hydraulic diameter PHE condenser with a corresponding chevron angle β = 63.26°. The saturation pressure P_{sat} was constant at 7.16 bar while the vapor quality x ran from 0.6 to 0.9. The mass flux G varied between 30 kg/m^{2}s and 65 kg/m^{2}s while the heat flux q" ranged from 11.5 kW/m^2 to 17.1 kW/m^2. No new correlations were reported for the two-phase multiplier ϕ_{LO}.

Shon et al. [5] studied the condensation of R1233zd(E) in a 3.32 mm hydraulic diameter and sixty-degree chevron angle PHE condenser. The saturation pressure P_{sat} varied between 2 and 3.5 bar, while the vapor quality x ran from 0.2 to 0.9. The mass flux G ranged from 19.9 kg/m^{2}s to 23.8 kg/m^{2}s while the heat flux q" varied between 2.5 kW/m^2 and 4.5 kW/m^2. A new friction factor correlation was reported, but no new two-phase multiplier ϕ_{LO} correlations were noted.

Soontarapiromsook et al. [6] investigated the condensation of R134a in a 5 mm hydraulic diameter and a sixty-five-degree chevron angle PHE condenser. The saturation temperature T_{sat} was 40°C and 50°C while the vapor quality x ran from 0.1 to 0.8. The mass flux G was 61 kg/m^{2}s and 89 kg/m^{2}s, while the heat flux q" went from 5 kW/m^2 to 15 kW/m^2. Soontarapiromsook et al. [6] investigated the effect of surface roughness on the condensation pressure drop but did not report any new two-phase ϕ_{LO} multiplier correlations.

Zhang et al. [7] reported adiabatic pressure drop data for the condensation of R134a, R1234Ze(E), and R245fa in a 3.4 mm hydraulic diameter and a sixty-five-degree chevron angle PHE condenser. The saturation temperature T_{sat} ranged from 30°C to 70°C. The vapor quality x ranged from 0.1 to 0.9, while the mass flux G was constant at 53 kg/m^{2}s. No new correlations were reported for the two-phase multiplier ϕ_{LO}.

Kwon et al. [8] studied the condensation of R1233zd(E) in a 3.88 mm hydraulic diameter and a sixty-degree chevron angle PHE condenser. The saturation pressure P_{sat} varied between 2 and 3 bar, while the vapor quality x ran from 0.2 to 0.9. The heat flux q" went from 2.5 bar to 4.5 bar, while the mass flux G ran from 13.3 kg/m^{2}s to 23.8 kg/m^{2}s. A new two-phase friction factor f_{TP} was reported. No new correlations were reported for the two-phase multiplier ϕ_{LO}.

Park and Kim [9] conducted condensation pressure drop experiments with R134a in a 5.6 mm hydraulic diameter and forty-five-degree chevron angle PHE condenser. The saturation temperature T_{sat} went from 30°C to 40°C, while the vapor quality x varied between 0 and 0.9. The mass flux G ran from 40 kg/m^{2}s to 80 kg/m^{2}s, while the heat flux q" went from 4 kW/m^2 to 8 kW/m^2. A new two-phase friction factor f_{TP} correlation was reported, but no new correlation was noted for the two-phase multiplier ϕ_{LO}.

Park et al. [10] investigated the condensation of R410A in a 5.6 mm hydraulic diameter and forty-five-degree chevron angle PHE condenser. The saturation temperature T_{sat} ran from 30°C to 40°C, while the vapor quality x went from 0 to 0.9. The heat flux q" varied between 4 kW/m^2 and 8 kW/m^2, while the mass flux G ranged from 40 kg/m^{2}s to 80 kg/m^{2}s. A new two-phase friction factor f_{TP} correlation was proposed, while no new correlations were reported for the two-phase multiplier ϕ_{LO}.

Tao et al. [11] reported adiabatic condensation pressure drop experiments with NH_3 in a 2.99 mm hydraulic diameter and a sixty-three-degree chevron angle PHE condenser. The saturation pressure P_{sat} ranged from 6.3 to 9.3 bar, while the vapor quality x ran from 0.05 to 0.65. The mass flux G went from 21 kg/m^{2}s to 78 kg/m^{2}s. No new correlations were reported.

Tao and Ferreira [12] studied the adiabatic condensation of NH_3 in a 2.99 mm hydraulic diameter and a sixty-three-degree chevron angle PHE condenser. The saturation pressure P_{sat} was constant at 6.9 bar, while the vapor quality x ranged from 0.1 to 0.65. The mass flux G ranged from 30 kg/m^{2}s to 71 kg/m^{2}s. A new Martinelli parameter-based two-phase multiplier correlation ϕ_{LO} was proposed.

Ko et al. [13] conducted condensation experiments with R124 in a 3.32 mm hydraulic diameter PHE condenser with thirty- and sixty-degree chevron angles, respectively. The vapor quality x went from 0.3 to 0.9, while the saturation pressure P_{sat} ranged from 5.6 to 7.9 bar. The heat flux q" ran from 2.5 kW/m^2 to 4.5 kW/m^2, while the mass flux G varied between 16 kg/m^{2}s and 26 kg/m^{2}s. A new two-phase friction factor f_{TP} correlation was proposed, but no new correlations were reported for the two-phase multiplier ϕ_{LO}.

Jung et al. [14] reported pressure drop data for the condensation of R124 in a 3.88 mm hydraulic diameter PHE condenser with thirty and sixty-degree chevron angles. The saturation pressure P_{sat} went from 7.2 bar to 9.2 bar, while the heat flux q" ran from 2.5 kW/m^2 to 4.5

kW/m^2. The mass flux G ranged from 2.5 kg/m^{2}s to 26.5 kg/m^{2}s, while the vapor quality x varied between 0.2 and 0.9. A new friction factor correlation was proposed regarding the equivalent Reynolds number Re_{eq} and the Weber number We. No new correlations were reported for the two-phase multiplier ϕ_{LO}.

Kwon et al. [15] studied the condensation of R1233zd(E) in a 4.2 mm hydraulic diameter and a sixty-degree chevron angle shell and plate condenser. The saturation pressure P_{sat} varied between 3 and 3.5 bar, while the vapor quality x went from 0.3 to 0.9. The heat flux q" ran from 1.5 kW/m^2 to 2.5 kW/m^2, while the mass flux G ranged from 10 kg/m^{2}s to 16 kg/m^{2}s. An equivalent Reynolds number Re_{eq}-based friction factor correlation was reported. However, no correlations were reported for the two-phase multiplier ϕ_{LO}.

Lee et al. [16] investigated the adiabatic condensation of R1234ze(E) in a 3.88 mm hydraulic diameter and sixty-degree chevron angle PHE condenser. The saturation temperature T_{sat} was constant at 15°C, while the vapor quality x ranged from 0.4 to 0.9. The mass flux G ran from 50 kg/m^{2}s to 130 kg/m^{2}s. No new correlations were reported.

Wang et al. [17] conducted adiabatic condensation studies with R365mfc in a mixed 27°/63° chevron angle PHE condenser. The saturation pressure P_{sat} was constant at 1.12 bar, while the mass flux G ran from 6.14 kg/m^{2}s to 44.56 kg/m^{2}s. The vapor quality x ranged from 0.58 to 0.92. No new correlations were reported.

Hu and Ma [18] studied the adiabatic condensation of a water-ethanol mixture in a 6 mm hydraulic diameter and a 60-degree chevron angle PHE condenser. The mass flux G varied between 5.9 kg/m^{2}s and 14.9 kg/m^{2}s, while the saturation pressure P_{sat} was 1.1 bar. The vapor quality x ran from 0 to 0.9. An equivalent Reynolds number Re_{eq}-based two-phase friction factor f_{TP} was developed. However, no new two-phase multiplier ϕ_{LO} correlations were proposed.

In most studies, a concerning trend emerged: the experimentally measured pressure drop was unexpectedly high, even at low mass flux G and liquid-only Reynolds number Re_{LO}. This was particularly evident in the PHE condenser tested by Hu and Ma [18], where the pressure drop reached a staggering 48,600 Pa at a meager liquid-only Reynolds number Re_{LO} = 19.9 and low mass flux of G = 11.9 kg/m^{2}s. Such a high-pressure drop at a low mass flow rate and Reynolds number is a significant concern, leading to increased refrigerant pressure drop and pump duty. To address this, future designs should consider deploying streamlined corrugations with a continuously varying chevron angle that gently guides the flow and reduces the pressure drop.

It's worth noting that, except for one study [12], none of the other investigations [2-11 and 13-18] reported any new modeling or correlations for the two-phase multiplier ϕ_{LO}. The Tao and Ferreira [12] correlation, while based on the Martinelli parameter and correctly modeling the liquid-only flow's contribution to the overall pressure drop, did not investigate other parameters such as the wetted perimeter, the effect of buoyancy, and slip on the phase-change pressure drop. Furthermore, the Tao and Ferreira [12] correlation was based on a limited amount of data, which restricts its range. This underscores the need for a universal correlation for the two-phase pressure drop multiplier to more accurately predict the contribution of the liquid and vapor phases to the overall pressure drop. The following section will explore these issues by modeling the compiled data [2-18].

Regression analysis and correlation development

The liquid-only friction pressure drop in Eq. (1) was calculated as follows:

$$\left(\frac{dP}{dZ}\right)_{LO} = \frac{2f_{LO}G^2}{d_h\rho_L} \tag{2}$$

The liquid-only friction factor f_{LO} was computed using the Moody [53] and Filonenko [54] formulas for laminar and turbulent flows, respectively.

$$f_{LO} = \frac{16}{Re_{LO}} (Re_{LO} \leq 2300) \quad (3)$$

$$f_{LO} = (1.82log_{10}Re_{LO} - 1.64)^{-2} (Re_{LO} > 2300) \quad (4)$$

A power-law model was chosen for empirical modeling based on the past use of various regression models such as ANOVA, ANCOVA, linear regression, non-linear regression, log-log regression, and others [1]. This led to the development of a novel predictive correlation for estimating the two-phase multiplier for condensing flows in PHEs, presented below in Eq. (5). This correlation has the potential to significantly enhance our understanding and prediction of the two-phase pressure drop multiplier, offering a promising direction for future research in this field.

$$\phi_{LO}^2 = 0.12Re_{LO}^{0.83}\left(\frac{\rho_L}{\rho_V}\right)^{0.0.036} X^{0.27}P_r^{-0.045}We^{-0.76}x^{0.047}\beta^{*0.49}\left(\frac{\mu_L}{\mu_V}\right)^{0.61} Bd^{0.73}T_r^{0.41} \quad (5)$$

Fig. 3 shows the iterative or trial-and-error regression process, while the corresponding sensitivity analysis is shown in Table 3. The iterative regression process started with a base correlation regarding the liquid-only Reynolds number Re_{LO}. The process involved incorporating relevant flow effects, such as the surface tension effects in terms of We, buoyancy effects in Bd, and other parameters in subsequent iterations until there was no further improvement in the R^2 value. The sensitivity analysis in Table 3 was obtained by varying one data value in Eq. (5) while keeping others constant. The study revealed that the slip effects represented by the density ratio $\left(\frac{\rho_L}{\rho_V}\right)$ was the most dominant. A ±10% variation in the density ratio produced a +16% to -15.2% error in the computed ϕ_{LO}^2. Another secondary flow effect, buoyancy, represented by the bond number Bd, was also significant. A ±10% variation in Bd yielded a ±7.2% error in the computed ϕ_{LO}^2. The competing effects of various secondary flows

were necessary to produce the optimal fit shown in Fig. 4. Removing any of those effects resulted in a poor R^2 value, as seen in Fig. 3. For example, including only the momentum effects in terms of Re_{LO} while ignoring secondary flows yielded an inferior R^2 value of 0.15.

As shown in Fig. 4, Eq. (5) fit 21.4% of the two-phase multipliers ϕ_{LO} computed from the compiled data [2-18] within ±10%, 54.1% within ±30%, and 72.3% within ±50%. The corresponding R^2 value was 0.73, while the MBD and RMSD values were -13.9% and 66.5%, respectively. The computed value of ϕ_{LO}^2 for the collected data [2-18] ranged from 33.4 to 16,654.3, suggesting from Eq. (1) that the contribution of the liquid phase to the overall pressure drop was less than 3%. This means the bulk of the total pressure drop was from the vapor phase. Equation (5) is valid for the liquid-only Reynolds number Re_{LO} = 13-7105, vapor quality 0 < x < 1, saturation pressure P_{sat} = 0.9-24.26 bar, heat flux q" = 0-20 kW/m^2, mass flux G = 2.5-150 kg/m^{2}s, hydraulic diameter d_h = 2.99-6.6 mm and chevron angle β = 30-65°.

Thermohydraulic interpretation of the condensation two-phase multiplier model

Equation (5) modeled the effect of the momentum or inertial forces in terms of the liquid-only Reynolds number, while the buoyancy effects were captured by the Bond number Bd. The computed Weber number We for most of the compiled data [2-18] was less than one, indicating that the surface tension effects were dominant, rendering drop formation impossible. This is reflected in the negative exponent for the Weber number We in Eq. (5). The exponent for the density ratio $\left(\frac{\rho_L}{\rho_V}\right)$ in Eq. (5) is not one. Further, since the liquid and vapor densities for all the tested refrigerants [2-18] are significantly different, Eq. (5) suggests a non-zero relative velocity at the liquid-vapor interface, leading to significant interface pressure drop during condensation. Despite the positive exponent of 0.95, the vapor quality x had minimal impact on the condensation pressure drop. This suggests that superheated vapors at the inlet or subcooled liquids at the exit may not increase the total condensation friction pressure drop and

the two-phase multiplier ϕ_{LO}. The dimensionless chevron angle β^* seems to have little impact on the condensation process, as evidenced by the negative exponent of -0.25. The viscosity ratio $\left(\frac{\mu_L}{\mu_V}\right)$ for the compiled data [2-18] was higher than one, indicating interfacial shear between the liquid and vapor phases due to kinetic mismatch in fluid friction.

Comparison with condensation correlations

The compiled data [2-18] was compared with some widely reported correlations for the two-phase multiplier ϕ_{LO}. Comparison with the widely reported Wang et al. [19] correlation is shown in Fig. 5. At an MBD of 82.4% and RMSD of 119.6%, the Wang et al. [19] correlation fit none of the two-phase multipliers computed from the data [2-18] within ±50%. The corresponding coefficient of correlation R^2 value was 0. The Wang et al. [19] correlation is based on an air-water mixture. Although that constitutes a two-phase mixture flow in a PHE, the lack of phase change, attendant latent heat release, and the corresponding pressure drop may have limited the accuracy of the correlation. It is suggested that the Wang et al. [19] correlation only be used for analyzing two-phase flows without phase change.

The Jiang and Bai [20] two-phase multiplier ϕ_{LO} correlation was also evaluated with the collected data [2-18]. As shown in Fig. 6, at an MBD of -1542% and RMSD of 9478%, the Jiang and Bai [20] correlation fit none of the two-phase multipliers ϕ_{LO} computed from the data [2-18[within ±50%. The corresponding R^2 value was zero. Similar to the Wang et al. [19] correlation, the Jiang and Bai [20] correlation was also based on an air-water mixture and lacked phase change phenomena. That could have resulted in a poor fit.

Comparison with the Shiomi et al. [21] correlation is shown in Fig. 7. At an MBD of -5161% and RMSD of 30,563%, the Shiomi et al. [21] correlation fit none of the two-phase multipliers ϕ_{LO} computed from the data [2-18] within ±50%. The corresponding R^2 value was

zero. The Shiomi et al. [21] correlation was also based on an air-water mixture with no phase change or condensation, which may have resulted in a poor fit.

Evaluation of the compiled data [2-18] with the Grabenstein et al. [22] correlation is shown in Fig. 8. At an MBD of 68.8% and RMSD of 168.5%, the Grabenstein et al. [22] correlation fit none of the two-phase multipliers ϕ_{LO} computed from the data [2-18] within ±50%. The corresponding R^2 value was zero. Although the Grabenstein correlation [22] was based on the condensation of R365mfc, it was a simplistic linear equation based on the Martinelli parameter X. Relevant flow modifiers such as the Bond number Bd to account for the buoyancy effects, Convection number Co, and density ratio $\left(\frac{\rho_L}{\rho_V}\right)$ to account for the interfacial slip and the Weber number We to determine if drop formation was possible were missing. Further, the Grabenstein et al. [22] correlation was based on limited data, limiting its effectiveness. These factors may have contributed to the poor fit.

Table 4 summarizes all the correlations in this section along with Eq. (5).

Meta-analysis of condensation in plate heat exchangers

Considering the wide range of available condensation pressure drop data [2-18] in PHEs, a statistical analysis was necessary to ascertain the reliability and consistency of the data before embarking on further studies using PHEs for condensation. To accomplish this, a meta-analysis of the collected data [2-18] was conducted using the CMA (Comprehensive meta-analysis) software developed by Biostat, Inc.

The condensation pressure drop data [2-18] were first reduced to the liquid-only two-phase multiplier ϕ_{LO} by using Eqs. (1-4). The uncertainty limits for the pressure drop provided by the authors [2-18] were used to calculate the uncertainty in the calculated two-phase multiplier ϕ_{LO} within the 95% confidence interval (CI). Since the individual studies were

conducted under widely different test conditions and refrigerants, a normalized variable that included all the dimensionless test variables was necessary for comparison. The control variable was set as $Re_{LO}^{0.83}\left(\frac{\rho_L}{\rho_V}\right)^{0.0.036} X^{0.27} P_r^{-0.045} We^{-0.76} x^{0.047} \beta^{*0.49} \left(\frac{\mu_L}{\mu_V}\right)^{0.61} Bd^{0.73} T_r^{0.41}$. This normalized variable included all the competing effects of buoyancy, surface tension, interfacial shear, slip, and fluid momentum. The two-phase multiplier ϕ_{LO} values at the control variable value of 3612 and the liquid-only Reynolds number Re_{LO} value of 958 were chosen for meta-analysis. Multiple data from each study at these control variables were averaged, and the standard deviation (STD) was calculated. Since it had the most data at the control variable, the Tao et al. [11] study was chosen as the control group. The remaining investigations comprised the study group [2-10, 12-18].

Figure 9 shows the condensation [2-18] two-phase multipliers ϕ_{LO} meta-analysis. Except for a few studies [13-15], the effect size for all the other studies crosses the null line. This indicates that most of the data [2-12, 16-18] is not statistically significant or relevant because the actual value of the two-phase multiplier ϕ_{LO} computed from that data falls within the 95% CI. The diamond representing the effect size of the pooled or compiled data [2-18] at the bottom of Fig. 9 crosses the null line with a positive bias. This means that PHE condensers can continue as meta-analysis was inconclusive. However, the pooled effect size tends towards the Tao and Ferreira [11] study, indicating that their data is statistically more reliable than the rest [2-10, 12-18]. Significant heterogeneity and inconsistency were detected in the pooled data [2-18]. The I^2 value was 91.48, while the Tau^2 value was 6.6. Both metrics indicate that different studies normalized to the same control variable and at the same liquid-only Reynolds number yielded vastly different two-phase multiplier ϕ_{LO} values while similar values were expected.

Ideally, I^2 should be less than 50, and Tau^2 should be zero for homogeneous and consistent data. Since the pooled effect size tends towards the control group [11], meta-analysis indicates that the two-phase multiplier ϕ_{LO} values computed from the Tao et al. [11] pressure drop data are more reliable and consistent in comparison to the study group [2-10, 12-18]. The combined effect size of all the studies [2-18] is shown in the cumulative meta-analysis in Fig. 10.

Evaluation of the condensation correlation

Equation (5) was evaluated with independent data [23-24] not used for the correlation development. This was to eliminate any bias and data redundancy. Had the source data [2-18] been used for evaluation, the fit quality would have been the same as Eq. (5) when it could be worse. Hence, a different data set [23-24] was necessary to verify Eq. (5). One of the widely used studies [15] was also added for adequate data volume. However, the data used for evaluation was from the PHE condensers in the study [15] and not the shell and plate condenser used for development. A brief description of the evaluation data [15, 23-24] ensues. Table 5 lists all the condensation evaluation data

Kwon et al. [15] reported pressure drop data for the condensation of R1233zd(E) in two 3.88 mm hydraulic diameter brazed plate heat exchangers with thirty-degree and sixty-degree chevron angles. The saturation pressure P_{sat} ran from 200 kPa to 300 kPa, while the vapor quality x ranged from 0.25 to 0.9. The mass flux G went from 13 kg/m^{2}s to 26.7 kg/m^{2}s, while the heat flux q" varied between 1.5 kW/m^2 and 4.5 kW/m^2.

Han et al. [23] investigated the condensation of R410A in brazed plate heat exchangers with chevron angles of 20°, 35°, and 45°. The hydraulic diameter was 5.1 mm. The saturation temperature T_{sat} was 20°C and 30°C, while the vapor quality x ran from 0.15 to 0.9. The heat flux q" went from 4.7 kW/m^2 to 5.3 kW/m^2, while the mass flux G ranged from 13-34 kg/m^{2}s.

Muller and Kabelac [24] studied the condensation of water vapor in a sixty-three-degree and twenty-seven-degree chevron angle PHE with a hydraulic diameter of 5.2 mm. The saturation pressure P_{sat} ranged from 534 kPa to 747 kPa, while the vapor quality x ran from 0.1 to 0.9. The heat flux q" went from 1.3 kW/m^2 to 114 kW/m^2, while the mass flux G varied between 5-55 kg/m^{2}s.

As shown in Fig. 11, at an MBD of 1.5% and RMSD of 36.7%, Eq. (5) fit 28.3% of the data [15, 23-24] within ±10%, 76.1% within ±30%, and 88.1% within ±50%. The corresponding R^2 value was 0.75. This excellent agreement with independent data [23-24] confirms the accuracy of Eq. (5).

Evaporators

One-thousand-eight-hundred-and-eighty-five data were collected from twenty-four references [25-48] for empirical modeling, analysis, and critique. Table 6 lists all the studies listed in this section. Table 7 presents the comparative analysis of the database.

Yan et al. [25] conducted pressure drop experiments with R134a in a 6.6 mm hydraulic diameter and a sixty-degree chevron angle PHE evaporator. The saturation pressure was 6.75 bar and 8 bar, respectively, while the heat flux q" was 11 kW/m^2 and 15 kW/m^2, respectively. The vapor quality x went from 0.1 to 0.9, while the mass flux G was 55 kg/m^{2}s and 70 kg/m^{2}s, respectively. No new two-phase multiplier ϕ_{LO} correlations were reported.

Kim and Lee [26] reported pressure drop data for the evaporation of R410A and R22 in a 4.3 mm hydraulic diameter PHE with chevron angle β ranging from 20° to 45°. The saturation temperature T_{sat} varied between 5°C and 15°C, while the mass flux G went from 13 kg/m^{2}s to 34 kg/m^{2}s. The vapor quality x ran from 0.15 to 0.95, while the heat flux q" went from 2.5 kW/m^2 to 8.5 kW/m^2. No new two-phase multiplier ϕ_{LO} correlation was reported.

Han et al. [27] studied the evaporation of R410A and R22 in a 5.1 mm hydraulic diameter PHE evaporator with the chevron angle β running from 20° to 45°. The mass flux G varied between 13 kg/m^{2}s and 34 kg/m^{2}s, while the saturation temperature T_{sat} ran from 5°C to 15°C. The vapor quality x went from 0.15 to 0.9, while the heat flux q" ran from 2.5 kW/m^2 to 8.5 kW/m^2. No new two-phase multiplier ϕ_{LO} correlations were reported.

Hsieh and Lin [28] investigated the evaporation of R410A in a 6.6 mm hydraulic diameter and a sixty-degree chevron angle PHE evaporator. The saturation pressure P_{sat} was 10.8 bar and 12.5 bar, respectively, while the vapor quality x ranged from 0.1 to 0.8. The mass flux G ran from 50 kg/m^{2}s to 100 kg/m^{2}s, while the heat flux q" went from 10 kW/m^2 to 20 kW/m^2. A new two-phase friction factor f_{TP} correlation was reported, but no new correlations were reported for the two-phase multiplier ϕ_{LO}.

Park and Kim [29] reported pressure drop data for the evaporation of R134a in a 5.6 mm hydraulic diameter and a forty-five-degree chevron angle PHE evaporator. The saturation temperature T_{sat} ranged from 0.01°C to 10°C, while the vapor quality x ran from 0 to 0.9. The heat flux q" was 4 kW/m^2 and 6 kW/m^2, while the mass flux G went from 40 kg/m^{2}s to 80 kg/m^{2}s. A new two-phase friction factor f_{TP} correlation was reported, but no new two-phase multiplier ϕ_{LO} correlations were presented.

Taboas et al. [30] studied the evaporation of an ammonia-water mixture in a 4 mm hydraulic diameter and a thirty-degree chevron angle PHE evaporator. The saturation pressure P_{sat} varied between 7 and 15 bar, while the heat flux q" ran between 20 kW/m^2 and 50 kW/m^2. The mass flux G went from 70 kg/m^{2}s to 140 kg/m^{2}s, while the vapor quality x ranged from 0 to 0.22. No new two-phase multiplier ϕ_{LO} correlations were reported.

Khan et al. [31] conducted evaporation experiments with NH_3 in a 4.4 mm hydraulic diameter and a thirty-degree chevron angle PHE evaporator. The saturation temperature T_{sat}

went from -25°C to -2°C, while the mean vapor quality x ran from 0.2 to 0.4. The heat flux q" ranged from 21 kW/m^2 to 44 kW/m^2, while the equivalent Reynolds number Re_{eq} varied between 1225 and 3000. A new two-phase friction factor f_{TP} correlation was proposed, but no new two-phase multiplier ϕ_{LO} correlations were presented.

Khan et al. [32] investigated the evaporation of NH_3 in a 4.4 mm hydraulic diameter and a sixty-degree chevron angle PHE evaporator. The mass flux G ranged from 8.5 kg/m^2s to 27 kg/m^2s, while the saturation temperature T_{sat} went from -25°C to -2°C. The heat flux q" ran from 21 kW/m^2 to 44 kW/m^2, while the equivalent Reynolds number Re_{eq} varied between 1387 and 2200. An equivalent-Reynolds number Re_{eq}-based two-phase friction factor correlation was proposed. However, no new two-phase multiplier ϕ_{LO} correlations were reported.

Vakili-Farahani et al. [33] reported adiabatic pressure drop data for the evaporation of R245fa in a 1.7 mm hydraulic diameter and a sixty-five-degree chevron angle PHE evaporator. The saturation temperatures T_{sat} ranged from 19°C to 35°C, while the mass flux G ran from 10 kg/m^2s to 40 kg/m^2s. The vapor quality x went from 0.05 to 0.8. The Lockhart and Martinelli [50] correlation was modified, and a new two-phase multiplier ϕ_{LO} correlation based on the turbulent Martinelli parameter $X_{turb, turb}$ was reported.

Lee et al. [34] studied the evaporation of water in a 5 mm hydraulic diameter and sixty-degree chevron angle PHE evaporator. The mass flux G ran from 14.5 kg/m^2s to 33.6 kg/m^2s, while the vapor quality x went from 0.09 to 0.6. The saturation pressure P_{sat} ranged from 1.12 bar to 1.21 bar, while the heat flux q" varied between 15 kW/m^2 and 30 kW/m^2. A new two-phase fiction factor f_{TP} correlation was proposed, but no new two-phase multiplier ϕ_{LO} correlations were proposed.

Khan et al. [35] conducted evaporation experiments with NH_3 in a 5.8 mm hydraulic diameter and 30°/60° unsymmetric chevron angle PHE evaporator. The saturation temperature T_{sat} ran from -25°C to -2°C, while the heat flux q" went from 21 kW/m^2 to 44 kW/m^2. The equivalent Reynolds number Re_{eq} ranged from 1225 to 3000, while the mean vapor quality x went from 0.5 to 0.8. A new two-phase friction factor f_{TP} correlation was reported, but no new two-phase multiplier ϕ_{LO} correlations were noted.

Khan et al. [36] investigated the evaporation of NH_3 in a 5.8 mm hydraulic diameter and 30°/60° unsymmetric chevron angle PHE evaporator at various oil concentrations. The saturation temperature T_{sat} ranged from -25°C to -2°C, while the mass flux G was constant at 6.5 kg/m^{2}s. The heat flux q" went from 21 kW/m^2 to 44 kW/m^2, while the equivalent Reynolds number Re_{eq} ran from 1225 to 3000. The mean vapor quality x varied between 0.5 and 0.8. New two-phase friction factor f_{TP} correlations were reported, but no new two-phase multiplier ϕ_{LO} correlations were noted.

Amalfi et al. [37] studied the evaporation of R245fa in a 1.7 mm hydraulic diameter and a sixty-five-degree chevron angle PHE evaporator. The mass flux G ranged from 10 kg/m^{2}s to 85 kg/m^{2}s, while the heat flux q" went from 0.225 kW/m^2 to 4.1 kW/m^2. The saturation temperature T_{sat} went from 19°C to 35°C, while the vapor quality x ran from 0.05 to 0.9. No new two-phase multiplier ϕ_{LO} correlations were reported.

Desideri et al. [38] reported adiabatic pressure drop data for R245fa and R1233zd(E) evaporation in a 3.4 mm hydraulic diameter and a sixty-five-degree chevron angle PHE evaporator. The saturation temperature T_{sat} ranged from 100°C to 130°C, while the average vapor quality x went from 0.3 to 0.7. The mass flux G ran from 68 kg/m^{2}s to 100 kg/m^{2}s. No new two-phase multiplier ϕ_{LO} correlations were reported.

Zhang et al. [39] conducted flow boiling experiments with R134a, R1234ze, and R1234yf in a 3.4 mm hydraulic diameter and a sixty-five-degree chevron angle PHE evaporator. The saturation temperature T_{sat} ranged from 60°C to 80°C, while the mass flux G went from 86 kg/m^{2}s to 137 kg/m^{2}s. The heat flux q" ran from 9.8 kW/m^2 to 36.8 kW/m^2, while the average vapor quality x varied between 0.5 and 1.0. A new two-phase friction factor f_{TP} correlation was proposed, but no new two-phase multiplier ϕ_{LO} correlations were proposed.

Kim et al. [40] investigated the evaporation of R1234ze(E) and R134a in two evaporators with chevron angles of 60° and 30°, respectively. The hydraulic diameter for both PHEs was 3.37 mm. The saturation temperature T_{sat} ranged from 5°C to 15°C, while the mass flux G went from 21 kg/m^{2}s to 58 kg/m^{2}s. The heat flux q" ran from 0.5 kW/m^2 to 10 kW/m^2, while the vapor quality x varied between 0.05 and 0.95. A new two-phase friction factor f_{TP} correlation was proposed, but no new two-phase multiplier ϕ_{LO} correlations were proposed.

Lee et al. [41] reported pressure drop data for the evaporation of R1233zd(E) in a 3.88 mm hydraulic diameter and a sixty-degree chevron angle PHE evaporator. The saturation temperature T_{sat} ranged from 60°C to 80°C, while the mass flux G ran from 32 kg/m^{2}s to 48 kg/m^{2}s. The heat flux q" went from 3.8 kW/m^2 to 10.4 kW/m^2, while the vapor quality x varied between 0.17 and 1.0. A liquid Reynolds number Re_L-based two-phase friction factor f_{TP} correlation was proposed, but no new two-phase multiplier ϕ_{LO} correlations were proposed.

Lee et al. [42] studied the evaporation of a mixture of R1234ze(E) and R32 in a 3.88 mm hydraulic diameter and sixty-degree chevron angle PHE evaporator. The saturation temperature T_{sat} was 5°C and 15°C, while the refrigerant mass flux G ranged from 32 kg/m^{2}s to 48 kg/m^{2}s. The heat flux q" was 6.45 kW/m^2 and 8.06 kW/m^2, while the vapor quality x went from 0.1 to 0.85. A new two-phase friction factor f_{TP} correlation was proposed, but no new two-phase multiplier ϕ_{LO} correlations were proposed.

Song et al. [43] investigated the evaporation of R245fa in two shell-and-plate heat exchangers with hydraulic diameters of 5 mm and 6 mm, respectively. The chevron angle β was 50°. The saturation temperature T_{sat} was 70°C, while the mass flux G was 30 kg/m^{2}s. The heat flux q" ranged from 6 kW/m^2 to 9 kW/m^2, while the vapor quality x ran from 0.1 to 0.8. An equivalent Reynolds number Re_{eq}-based two-phase friction factor f_{TP} was reported, but no new two-phase multiplier ϕ_{LO} correlations were proposed.

Soontarapiromsook et al. [44] reported pressure drop data for the evaporation of R134a in PHE evaporators with various surface roughnesses. The hydraulic diameter of all the PHEs was 5 mm, while the corresponding chevron angle β was 65°. The saturation temperature T_{sat} ranged from 10°C to 20°C, while the mass flux G went from 67 kg/m^{2}s to 96 kg/m^{2}s. The heat flux q" ran from 10°C to 20°C, while the vapor quality x varied between 0.1 and 0.8. A new two-phase friction factor f_{TP} correlation was reported, but no new two-phase multiplier ϕ_{LO} correlations were noted.

Jo et al. [45] conducted evaporation experiments with R1234ze(E) in a 3.315 mm hydraulic diameter and a sixty-degree chevron angle PHE evaporator. The vapor quality x ranged from 0.18 to 0.9, while the mass flux G ran from 20 kg/m^{2}s to 40 kg/m^{2}s. The heat flux q" went from 2.3 kW/m^2 to 6.9 kW/m^2, while the saturation temperature T_{sat} varied between 7°C and 20°C. An equivalent Reynolds number Re_{eq}-based two-phase friction factor f_{TP} correlation was reported, but no new two-phase multiplier ϕ_{LO} correlations were noted.

Zhang and Haglind [46] studied the evaporation of R134a, R236fa, R245fa, R1234ze(E), R1233zd(E), propane, and isobutane in a 3.4 mm hydraulic diameter and a sixty-five-degree chevron angle PHE evaporator. The saturation temperature T_{sat} ran from 55°C to 141°C, while the mass flux G went from 52 kg/m^{2}s to 137 kg/m^{2}s. The vapor quality x ranged from 0 to 0.5. No new two-phase multiplier ϕ_{LO} correlations were reported.

Yang et al. [47] investigated the evaporation of R32 in a 3.88 mm hydraulic diameter and a sixty-degree-chevron angle PHE evaporator. The saturation temperature T_{sat} was 5°C and 15°C, while the mass flux G went from 50 kg/m^{2}s to 90 kg/m^{2}s. The heat flux q" was constant at 6.45 kW/m^2, while the vapor quality x ranged from 0.01 to 0.9.

Huang et al. [48] reported pressure drop data for the evaporation of a mixture of R134a and R245fa in a 2 mm hydraulic depth and a sixty-five-degree chevron angle PHE evaporator. The heat flux q" went from 15.2 kW/m^2 to 39.7 kW/m^2, while the mass flux G ran from 103 kg/m^{2}s to 137 kg/m^{2}s. The average vapor quality x ranged from 0.325 to 0.715, while the saturation pressure P_{sat} varied between 17.9 and 27.6 bar. A new friction factor correlation was reported, but no two-phase multiplier ϕ_{LO} correlations were noted.

The following section presents the empirical modeling, critique, and analysis of the compiled data [25-48].

Regression analysis and correlation development

The evaporation pressure drop data [25-48] were reduced to the two-phase multipliers ϕ_{LO} using Eqs. (1-4). The computed two-phase multipliers ϕ_{LO} were then modeled using various regression tools such as ANOVA, ANCOVA, linear and nonlinear regression, and power law regression. The power law model in Eq. (6) best fits all the models.

$$\phi_{LO}^2 = 0.14 Re_{LO}^{0.82} Co^{-0.24} Bo^{0.02} X^{0.26} P_r^{-0.33} Bd^{0.5} We^{-0.55} \beta^{*-0.19} T_r^{0.88} \left(\frac{\rho_L}{\rho_V}\right)^{-0.05} \left(\frac{\mu_L}{\mu_V}\right)^{0.44} \quad (6)$$

Like the condensation regression, Fig. 12 depicts the iterative evaporation regression process and the selection of relevant flow modifiers and their impact on the R^2 value. The sensitivity analysis in Table 8 indicates that the reduced temperature T_r was the most dominant parameter in Eq. (6). Secondary flow effects, such as the buoyancy effects at ±5% and surface tension effects at -5.1% to +6%, were not negligible.

As shown in Fig. 13, at an MBD of -10.1% and RMSD of 73.5%, Eq. (6) fit 15.5% of the two-phase multipliers ϕ_{LO} computed from the data [25-48] within ±10%, 49.3% within ±30%, and 71.2% within ±50%. The corresponding R^2 value was 0.79. Based on the computed values of the two-phase multiplier ϕ_{LO}, the maximum contribution of the liquid phase to the total evaporation pressure drop calculated from Eq. (1) was 15.6%. Correspondingly, the maximum contribution of the vapor phase to the total pressure drop was 84.4%. This suggests a rapid vaporization of the liquid over a short length of the PHE. Equation (6) is valid for the liquid-only Reynolds number Re_{LO} = 19-4870, saturation pressure P_{sat} = 0.165-27.63 bar, heat flux q" = 0-49.1 kW/m^2, mass flux G = 5.5-140 kg/m^{2}s, vapor quality 0 < x < 1, hydraulic diameter d_h = 1.7-15 mm, chevron angle β = 20-65°, and reduced pressure P_r = 0.005-0.65.

Thermohydraulic interpretation of the evaporation two-phase multiplier model

The exponent of the convection coefficient Co, which is proportional to the slip velocity, in Eq. (6) was non-zero and positive. Further, the density ratio $\left(\frac{\rho_L}{\rho_v}\right)$ for the compiled evaporation data [25-48] was much higher than one. This indicates slip and shear between the liquid and vapor phases at the interface due to the momentum mismatch arising from the density difference at the interface. This interfacial shear may also have increased the pressure drop and the two-phase multiplier ϕ_{LO} values. Additional research is necessary to investigate the specific contribution of the interfacial shear and slip to the evaporation pressure drop. The exponent for the Bond number Bd was also non-zero and positive, indicating a direct correlation to the computed two-phase multiplier ϕ_{LO}. This suggests that the buoyancy forces were relevant during evaporation in the PHEs. The computed Weber number We for the bulk of the evaporation data [25, 28-30, 38-39, 41, 44,46-48] was greater than one, indicating the surface tension effects were low enough for bubble formation during evaporation. The negative exponent of the Boiling parameter Bo suggests that the impact of convective boiling

was negligible compared to pool boiling. The dynamics between the competing thermo-hydraulic effects, such as buoyancy vs. surface tension, convective boiling vs pool boiling, etc., were captured in Eq. (6), resulting in the overall fit.

Comparison with evaporation correlations

The computed two-phase multipliers ϕ_{LO} obtained from the pressure-drop data [25-48] were tested with some widely reported correlations. Comparison with the Vakili-Farahani et al. [33] correlation is shown in Fig. 14. At an MBD of -505.6% and RMSD of 8579%, the Vakili-Farahani et al. [33] correlation fit 2.5% of the evaporation two-phase multipliers ϕ_{LO} computed from the data [25-48] within 10%, 8.5% within ±30%, and 21% within ±50%. The R^2 value was zero. The Vakili-Farahani et al. [33] correlation was based on the evaporation of R245fa and was a modification of the Lockhart and Martinelli [50] correlation and was based on turbulent liquid and vapor flow. The evaporation pressure drop data [25-48] spans the laminar-transition-turbulent flow regimes with the liquid Reynolds number Re_{LO} ranging from 19 to 4870. The lack of the proper Martinelli parameter X in the laminar and transition regimes for liquid and vapor flow may have caused the poor fit. The Vakili-Farahani et al. [33] correlation did not consider the effects of interfacial slip and shear, buoyancy, and surface tension. This may have also resulted in a poor fit.

The correlation between the Taboas et al. [49] and the evaporation data [25-48] was also evaluated. As shown in Fig. 15, at an MBD of -399.3% and RMSD of 7850%, the Taboas et al. [49] correlation fit 1.5% of the two-phase multipliers ϕ_{LO} computed from the data [25-48] within ±10%, 3.9% within ±30%, and 7.4% within ±50%. The R^2 value was zero. The Taboas et al. [49] correlation was only valid for vapor quality x less than 0.22. The vapor quality x for the current analysis ran from zero to one. Consequently, the Taboas et al. [49] correlation was not valid for a significant portion of the flow range. This may have contributed

to the poor fit. The Taboas et al. [49] correlation also modified the Lockhart and Martinelli [50] correlation and did not have the slip, buoyancy, and surface tension effects. That may also have resulted in a poor fit.

The seminal work of Lockhart and Martinelli [50] was also compared with the data [25-48]. As shown in Fig. 16, at an MBD of -36,050% and RMSD of 168,698%, the Lockhart and Martinelli [50] correlation fit 0.75% of the two-phase multipliers ϕ_{LO} computed from the evaporation pressure drop data [25-48] within ±10%, 1.8% within ±30%, and 4.3% within ±50%. The R^2 value was zero. Although authoritative, the Lockhart and Martinelli [50] correlation is based on oil-air, water-air, benzene-air, and kerosene-air mixtures with no phase change. Several features, such as nucleation or drop formation, latent heat release or absorption, and condensation or evaporation due to interfacial shear, were absent in their data and analysis. This may have resulted in a poor fit. It is suggested that although the Lockhart and Martinelli [50] model is a good starting point, relevant phase-change modifiers have to be included for accuracy.

Comparison with the Nilpueng and Wongwises [51] correlation is shown in Fig. 17. At an MBD of -268.7% and RMSD of 1117%, the Nilpueng and Wongwises [51] correlation fit 0.2% of the two-phase multipliers ϕ_{LO} computed from the data [25-48] within ±10%, 0.9% within ±30%, and 2.1% within ±50%. Their correlation is based on an air-water mixture with no evaporation. The lack of phase-change data may have caused the poor fit. The Nilupeng and Wongwises [51] correlation is a simple linear function of the Martinelli parameter X without any slip, buoyancy, or surface tension effects. This may have also yielded a poor fit.

Table 9 lists all the correlations cited in this section along with Eq. (6).

Meta-analysis of evaporation in plate heat exchangers

Meta-analysis was done on the evaporation data [25-48] using the CMA software. To normalize the pressure drop data from studies [25-48] with different test conditions, the non-dimensional control parameter was chosen as $Re_{LO}^{0.82} Co^{-0.24} Bo^{0.02} X^{0.26} P_r^{-0.33} Bd^{0.5} We^{-0.55} \beta^{*-0.19} T_r^{0.88} \left(\frac{\rho_L}{\rho_V}\right)^{-0.05} \left(\frac{\mu_L}{\mu_V}\right)^{0.44}$. The control parameter includes all the relevant flow variables influencing the two-phase multiplier ϕ_{LO} and the phase-change pressure drop. For meta-analysis, the value of the control parameter was set as 199.98. Only the two-phase multipliers ϕ_{LO} at this control value were chosen for meta-analysis. Further, the corresponding liquid-only Reynolds number Re_{LO} for the selected data [25-48] was 618.5. Consequently, only the computed two-phase multipliers ϕ_{LO} at a control value of 199.98 and liquid-only Reynolds number Re_{LO} = 618.5 were chosen for evaluation. This ensured uniformity in the data taken from various sources [25-48]. Although the individual test conditions and fluids were different [25-48], the normalization of the multiple parameters to dimensionless parameters, such as the control variable, liquid-only Reynolds number Re_{LO}, and the two-phase multiplier ϕ_{LO}, ensured similitude and a basis for comparison.

Similar to a meta-analysis on the condensation data [2-18], the effect size for the Forest plot was computed for the STDs of the data [25-48] and at 95% CI. Meta-analysis of the two-phase multipliers ϕ_{LO} computed from the evaporation pressure drop data is shown in Fig. 18. Except for the Hsieh and Lin [28], Desideri et al. [38], Zhang et al. [39], and the Zhang and Haglind [46] studies, the effect size of the computed two-phase multipliers ϕ_{LO} does not cross the null line. This means that the bulk of the evaporation data [25-27, 29-37, 41-48] is statistically significant and relevant as the true mean of the two-phase multiplier ϕ_{LO} is not within the 95% CI band. The resultant effect size depicted by the pooled diamond at the bottom of the figure lies between the lower limit of 32.1 and the upper limit of 38.7. This indicates

that the results of our meta-analysis are not only statistically significant but also positive, underscoring the strong recommendation for using PHE evaporators in the process industry.

The I^2 value was 99.8, and the Tau^2 value was 62.2. This indicates substantial heterogeneity and inconsistency in the data [25-48]. Ideally, the I^2 value should be less than fifty, and the Tau^2 value should be zero for homogenous and consistent data. This indicates that all the normalized and standardized data at the same similarity or control variable and liquid-only Reynolds number Re_{LO} yielded widely different pressure drops and two-phase multipliers ϕ_{LO} when they should have yielded near identical values. The Huang et al. [48] study was chosen as the control group as it had the maximum data at the control point of 199.98 and liquid-only Reynolds number Re_{LO} of 618.5. Since the pooled effect size tends towards the control group and does not cross the null line, it can be concluded that the Huang et al. [48] study was more reliable, homogenous, and consistent than the investigations in the study group [25-47]. The cumulative meta-analysis is shown in Fig. 19.

Validation of the correlation for evaporation

Equation (6) was also validated with one independent data [52] set. This was done to avoid any bias. Had all the data [25-48] used for developing Eq. (6) been used for validation, the resulting fit would have been identical to the values presented in Fig 13. Only by deploying unrelated data within the range of validity of Eq. (6) can its accuracy and reliability be judged accurately. Since only one independent data set [52] could be found, the widely reported data by Amalfi et al. [37] used for development was also included in the validation database.

Amalfi et al. [37] studied the evaporation of R245fa in a 1.7 mm hydraulic diameter and a sixty-five-degree chevron angle PHE evaporator. The mass flux G ranged from 10 kg/m^2s to 85 kg/m^2s, while the heat flux q" went from 0.225 kW/m^2 to 4.1 kW/m^2. The

saturation temperature T_{sat} went from 19°C to 35°C, while the vapor quality x ran from 0.05 to 0.9. No new two-phase multiplier ϕ_{LO} correlations were reported.

Longo et al. [52] reported pressure drop data for the evaporation of R1234ze(Z) and R1233zd(E) in a 4 mm hydraulic diameter and a sixty-five-degree chevron angle PHE evaporator. The saturation temperature T_{sat} ranged from 29.9°C to 40.2°C, while the mass flux G ran from 10.8 kg/m^{2}s to 62.3 kg/m^{2}s. The heat flux q" went from 2.3 kW/m^2 to 21.6 kW/m^2, while the vapor quality x at the inlet varied between 0.19 and 0.26. No new two-phase multiplier ϕ_{LO} correlations were reported.

Table 10 lists the evaluation data. As shown in Fig. 20, at an MBD of -30.1%, RMSD of 49.8%, and R^2 value of 0.67, Eq. (6) fit 12.2% of the evaluation data [37, 52] data within ±10%, 37.8% within ±30%, and 69.5% within ±50%. This excellent fit validates the accuracy and reliability of Eq. (6).

Conclusions

This article empirically modeled the condensation [2-18] and evaporation [25-48] pressure drop in PHEs and presented predictive correlations for estimating the two-phase multiplier ϕ_{LO}. The two-phase multiplier will yield the relative contributions of the liquid and vapor phase flows to the overall pressure drop. The predictive correlations for ϕ_{LO}, Eq. (5) for condensation, and Eq. (6) for evaporation were compared with widely reported correlations and evaluated with independent data. Some of the significant findings of this study are as follows:

1. Very few predictive correlations [12, 19-22, 33-34, 49-51] for the two-phase multiplier ϕ_{LO} in PHEs were detected in the literature. Most of the modeling is focused on estimating the two-phase friction factor f_{TP}. Although the two-phase friction factor is a valuable metric for evaluating the total pressure drop in a PHE, it cannot assess the

relative contributions of the liquid and vapor phases to the overall pressure drop. Hence, more predictive models for the two-phase multiplier are necessary to improve the understanding of the hydraulics in PHEs.

2. Except for the Grabenstein et al. [22] correlation for condensation and the Vakili-Farahani et al. [33] and Taboas et al. [49] correlations for evaporation, none of the other correlations for estimating the two-phase multiplier ϕ_{LO} were based on phase-change processes. Predictive models based solely on two-phase mixtures such as air-water may be easier but have no value in modeling condensation and evaporation in PHEs.
3. Robust modeling (empirical, statistical, computational, numerical, etc.) of phase-change processes in PHEs involving the release or absorption of latent heat and attendant pressure drop is necessary. Models that merely modify the Martinelli constant C tend to be poor fits to the data [2-18] and [25-48]. The condensation correlation Eq. (5) presented in this article is valid for the liquid-only Reynolds number Re_{LO} = 13-7105, vapor quality $0 < x < 1$, saturation pressure P_{sat} = 0.9-24.26 bar, heat flux q" = 0-20 kW/m^2, mass flux G = 2.5-150 kg/m^{2}s, hydraulic diameter d_h = 2.99-6.6 mm and chevron angle β = 30-65°. Similarly, the evaporation correlation Eq. (6) is valid for the liquid-only Reynolds number Re_{LO} = 19-4870, saturation pressure P_{sat} = 0.165-27.63 bar, heat flux q" = 0-49.1 kW/m^2, mass flux G = 5.5-140 kg/m^{2}s, vapor quality $0 < x < 1$, hydraulic diameter d_h = 1.7-15 mm, chevron angle β = 20-65°, and reduced pressure P_r = 0.005-0.65.
4. The two-phase multiplier ϕ_{LO} values suggest that the maximum contribution of the liquid phase to the overall pressure was 3% for the condensation studies [2-18] and 15.6% for evaporation studies [25-48]. Since these estimates were primarily based on global measurements, detailed local investigations that measure the local liquid flow in PHEs are necessary. In particular, pressure taps should be located on PHEs where

intense local flooding of the condensate or liquid is observed to measure the static pressure variation. The acceleration or deceleration of that fluid slug may add to the friction pressure drop.

5. Refrigerants or refrigerant mixtures with liquid-to-vapor density and viscosity ratios closer to unity must be selected. Significant differences in the liquid and vapor phase densities and viscosities lead to kinetic mismatch at the interface, increasing the local shear, interfacial slip, and overall pressure drop. A ±10% variation in the density ratio yielded a 16% to -15.2% error in the computed condensation two-phase multiplier, indicating the significance of slip effects and the need for refrigerants with a density ratio closer to unity.
6. It is also recommended that the plate corrugations be continuously varying instead of fixed. The current herringbone-type serrations on the plates promote uneven turbulent fluid mixing and higher pressure drops. Corrugations that follow the flow streamlines, such as a sinusoidal or wavy path with continuously varying chevron angles, may promote better turbulence and uniform wetting of the plates.

Nomenclature

A	Area of cross section (m^2)
A_P	PHE heat transfer area (m^2)
ANOVA	Analysis of variance
ANCOVA	Analysis of Covariance
Bo	Boiling parameter (-) $\left(\frac{q"}{Gi_{fg}}\right)$
Bd	Bond number (-) $\left(\frac{g(\rho_L-\rho_v)d_h^2}{\sigma}\right)$
C	Martinelli constant
CI	Confidence interval
C_L	Liquid phase Martinelli constant (-)
CMA	Comprehensive meta-analysis
Co	Convection number (-) $\left(\frac{\rho_v}{\rho_L}\right)^{0.5}\left(\frac{1-x}{x}\right)^{0.8}$
C_V	Vapor phase Martinelli constant (-)
d_h	Hydraulic diameter (m)
exp	Experimental value
f( )	Function
f_{LO}	Liquid-only Fanning friction factor (-)
f_{TP}	Two-phase Fanning friction factor (-) $(f_{TP} = \frac{\Delta P\ \rho_m d_h}{2G^2 Z})$
g	Gravitational acceleration (9.81 m/s^2)

G	Mass velocity $\left(\frac{\dot{m}}{A}\right)$ (kg/m^{2}s)
G_{eq}	Equivalent mass flux $G(1-x)+x\left(\frac{\rho_L}{\rho_V}\right)^{0.5}$ (kg/m^{2}s)
G_L	Liquid mass flux G (1 - x) (kg/m^{2}s)
G_V	Vapor mass flux Gx (kg/m^{2}s)
HX	Heat exchanger
i_{fg}	Latent heat of vaporization (kJ/Kg K)
I^2	Heterogeneity index (I-squared)
$\dot{m}$	Mass flow rate (kg/s)
MBD	Mean bias deviation $\frac{1}{N}\sum\left(\frac{exp-pred}{exp}\right)$
N	Count; sample size; the number of data
P_{crit}	Critical pressure (Pa)
P_r	Reduced pressure (-) $\left(\frac{P_{sat}}{P_{crit}}\right)$
P_{sat}	Saturation pressure
ΔP	Pressure drop (Pa)
$\frac{dP}{dZ}$	Pressure gradient (Pa/m)
$\left(\frac{dP}{dZ}\right)_{TP}$	Two-phase pressure gradient (Pa/m)
$\left(\frac{dP}{dZ}\right)_{LO}$	Liquid-only pressure gradient (Pa/m)

PHE	Plate heat exchanger
pred	Predicted value
q”	Heat flux (W/m^2)
Re_{eq}	Equivalent Reynolds number (-) $\left(\frac{G_{eq} d_h}{\mu_L}\right)$
Re_L	Liquid Reynolds number (-) $\left(\frac{G d_h}{\mu_L}\right)$
Re_{LO}	Liquid-only Reynolds number (-) $\left(\frac{G(1-x) d_h}{\mu_L}\right)$
Re_{mix}	Mixture Reynolds number (-) $\left(\frac{(G_L+G_V) d_h}{(1-x)\mu_L+x\mu_V}\right)$
Re_{TP}	Two-phase Reynolds number (-) $\left(\frac{G d_h}{\mu_{TP}}\right)$
Re_V	Vapor Reynolds number (-) $\left(\frac{G d_h}{\mu_V}\right)$
RMSD	Root mean square deviation $\sqrt{\frac{1}{N}\sum\left\{\left(\frac{exp-pred}{exp}\right)^2\right\}}$
R^2	Coefficient of determination
STD	Standard deviation
T_r	Reduced temperature (-) $\left(\frac{T_{sat}}{T_{crit}}\right)$
T_{crit}	Critical temperature (K)
T_{sat}	Saturation temperature (K)
Tau^2	Absolute value of true variance (Heterogeneity)
We	Weber number (-) $\left(\frac{G^2 d_h}{\sigma \rho_L}\right)$

x Vapor quality (-)

Z Length (m)

Z_P Port length of the PHE (m)

Greek Symbols

β Chevron angle (°)

β* $\left(\frac{\beta}{180}\right)$ (rad)

X $\left(\left(\frac{1-x}{x}\right)\left(\frac{\rho_V}{\rho_L}\right)\left(\frac{\mu_L}{\mu_v}\right)\right)^{\frac{1}{2}}$ (for $Re_{LO} < 2000$ and $Re_V < 2000$)

$\sqrt{Re_V^{-0.8}\left(\frac{C_L}{C_v}\right)\left(\frac{\dot{m}_L}{\dot{m}_v}\right)\left(\frac{\rho_L}{\rho_v}\right)\left(\frac{\mu_L}{\mu_v}\right)}$ ($C_L = 16$, $C_V = 0.046$ for $Re_{LO} < 1000$ and $Re_v > 2000$; $C_L = 0.046$ and $C_V = 16$ for $Re_{LO} > 2000$ and $Re_v < 1000$; $\dot{m}_L = G(1-x)A$ and $\dot{m}_v = GxA$)

$\left(\frac{1-x}{x}\right)^{0.8}\left(\frac{\rho_v}{\rho_L}\right)^{0.5}\left(\frac{\mu_L}{\mu_V}\right)^{0.1}$ (for $Re_{LO} > 2000$ and $Re_V > 2000$)

μ Dynamic viscosity (Pa.s)

μ_{TP} Two-phase dynamic viscosity (Pa.s) $\rho_m\left(x\left(\frac{\mu_V}{\rho_V}\right) + (1-x)\left(\frac{\mu_L}{\rho_L}\right)\right)$

ϕ_{LO} Liquid-only two-phase multiplier

ϕ_L Liquid-phase two-phase multiplier

ρ Density (kg/m^3)

ρ_m Mean density (kg/m^3) $\left[\left(\frac{1-x}{\rho_L}\right) + \left(\frac{x}{\rho_V}\right)\right]^{-1}$

σ	Surface tension (N/m)

Subscripts

crit	Critical parameter
eq	Equivalent
h	Hydraulic parameter
L	Liquid
LO	Liquid-only
m	mean value
mix	Mixture value
P	Plate parameter
r	Reduced parameter
sat	Saturated state
TP	Two-phase flow parameter
turb, turb	turbulent liquid, and turbulent vapor flow parameter
V	Vapor

Acknowledgments

The authors thank the University of Pretoria and Vellore Institute of Technology for the research resources. No conflicts of interest are reported.

References

[1] Y. Mukkamala and J. Dirker, “Empirical modeling and meta-analysis of heat transfer in plate heat exchangers,” *Heat Transf. Eng.*, vol. 45, no. 16, 2024. DOI: 10.1080/01457632.2023.2260524.

[2] Y.Y. Yan, H.C. Lio, and T.F. Lin, “Condensation heat transfer and pressure drop of refrigerant R-134a in a plate heat exchanger”, *Int. J. Heat Mass Transf*., vol. 42, no. 6, pp. 993-1006, Mar. 1999. DOI: 10.1016/S0017-9310(98)00217-8.

[3] W.S. Kuo, Y.M. Lie, Y.Y. Hsieh, and T.F. Lin, "Condensation heat transfer and pressure drop of refrigerant R-410A flow in a vertical plate heat exchanger", *Int. J. Heat Mass Transf.,* vol. 48, no. 25-26, pp. 5205-5220, Dec. 2005. DOI: 10.1016/j.ijheatmasstransfer.2005.07.023.

[4] E.M. Djordjevic, S. Kabelac, and S.P. Serbanovic, "Heat transfer coefficient and pressure drop during refrigerant R-134a condensation in a plate heat exchanger", *Chem. Pap.*, vol. 62, no. 1, pp. 78-85, 2008. DOI: 10.2478/s11696-007-0082-8.

[5] B.H. Shon, C.W. Jung, O.J. Kwon, C.K. Choi, and Y.T. Kang, "Characteristics on condensation heat transfer and pressure drop for a low GWP refrigerant in brazed plate heat exchanger," *Int. J Heat Mass Transf.,* vol. 122, pp. 172-1282, Jul. 2018. DOI: 10.1016/j.ijheatmasstransfer.2018.02.077.

[6] J. Soontarapiromsook, O. Mahian, A.S. Dalkilic, and S. Wongwises, "Effect of surface roughness on the condensation of R-134a in vertical chevron gasketed plate heat exchangers", *Exp. Therm. Fluid Sci.,* vol. 91, pp. 54-63, Feb. 2018. DOI: 10.1016/j.expthermflusci.2017.09.015.

[7] J. Zhang, M.R. Kaern, T. Ommen, B. Elmegaard, and F. Haglind, "Condensation heat transfer and pressure drop characteristics of R134a, R1234ze(E), R245fa, and R1233zd(E) in

a plate heat exchanger", *Int. J Heat Mass Transf.*, vol. 128, pp. 136-149, Jan. 2019. DOI: 10.1016/j.ijheatmasstransfer.2018.08.124.

[8] O.J. Kwon, B.H. Shon, and Y.T. Kang, "Experimental investigation on condensation heat transfer and pressure drop of a low GWP refrigerant R-1233zd(E) in a plate heat exchanger", *Int. J Heat Mass Transf.*, vol. 131, pp. 1009-1021, Mar. 2019. DOI: 10.1016/j.ijheatmasstransfer.2018.11.114.

[9] J.H. Park and Y.S. Kim, "Condensation heat transfer and pressure drop of R134a in the oblong shell and plate heat exchanger", *Int. J Air-Cond. Refrig.*, vol. 12, no. 3, pp. 158-167, 2004.

[10] J.H. Park, Y.C.H. Kwon, and Y.S. Kim, "Experimental study on R-410A condensation and heat transfer and pressure drop characteristics in oblong shell and plate heat exchanger", presented at the Int. Refrig. and Air-Cond. Conf., Purdue, USA, article no. R061, 8 pages, Jul. 12-15, 2004.

[11] X. Tao, E. Dahlgren, M. Leichsenring, and C.A.I. Ferreira, "NH_3 condensation in a plate heat exchanger: Experimental investigation on flow patterns, heat transfer and frictional pressure drop", *Int. J Heat Mass Transf.*, vol. 151, article no. 119374, Apr. 2020. DOI: 10.1016/j.ijheatmasstransfer.2020.119374.

[12] X. Tao and C.A.I. Ferreira, "NH_3 condensation in a plate heat exchanger: Flow pattern based models of heat transfer and frictional pressure drop", *Int. J Heat Mass Transf.*, vol. 154, article no. 119774, Jun. 2020. DOI: 10.1016/j.ijheatmasstransfer.2020.119774.

[13] Y.M. Ko, J.H. Jung, S. Sohn, C.H. Song, and Y.T. Kang, "Condensation heat transfer performance and integrated correlations of low GWP refrigerants in plate heat exchangers," *Int. J Heat Mass Transf.*, vol. 177, article no 121519, 13 pages, Oct. 2021. DOI: 10.1016/j.ijheatmasstransfer.2021.121519.

[14] J.H. Jung, Y.M. Ko, and Y.T. Kang, "Condensation heat transfer characteristics and energy conversion performance analysis for low GWP refrigerants in plate heat exchangers," *Int. J Heat Mass Transf.*, vol. 166, article no. 120727, 12 pages, Feb. 2021. DOI: 10.1016/j.ijheatmasstransfer.2020.120727.

[15] O.J. Kwon, J.H. Jung, and Y.T. Kang, "Development of experimental Nusselt number and friction factor correlations for condensation of R-1233zd(E) in plate heat exchangers", *Int. J Heat Mass Transf.*, vol. 158, article no. 120008, 15 pages, Sep. 2020. DOI: 10.1016/j.ijheatmasstransfer.2020.120008.

[16] D.C. Lee, S. Yun, J.Y. Choi, and Y. Kim, "Flow patterns and heat transfer characteristics of R-1234ze(E) for downward condensation in a plate heat exchanger", *Int. J Heat Mass Transf.*, vol. 175, article no. 121373, 16 pages, Aug. 2021. DOI: 10.1016/j.ijheatmasstransfer.2021.121373.

[17] R. Wang, Y. Zhang, W. Li, and S. Kabelac, "Flow pattern, heat transfer and frictional pressure drop investigation of R365mfc condensation in a micro-structured corrugated gap with mixed angles", *Appl. Therm. Eng.*, vol. 201, part B, article no. 117812, 13 pages, Jan. 2022. DOI: 10.1016/j.applthermaleng.2021.117812.

[18] S. Hu and X. Ma, "Experimental study of pressure drop during water-ethanol condensation in a vertical plate heat exchanger," *Heat Mass Transf.*, vol. 58, pp. 1289-1302, Aug. 2022. DOI: 10.1007/s00231-022-03175-5.

[19] K. Wang, J. Chen, P. Wu, H. Zhong, and L. Liu, "The characteristics of flow patterns in the shell-and-plate heat exchanger," *Int. J. Refrig.*, vol. 152, pp. 315-330, Aug. 2023. DOI: 10.1016/j.ijrefrig.2023.04.024.

[20] C. Jiang and B. Bai, "Flow patterns and pressure drop of downward two-phase flow in a capsule-type plate heat exchanger," *Exp. Therm. Fluid Sci.,* Vol. 103, pp. 347-354, May 2019. DOI: 10.1016/j.expthermflusci.2019.01.026.

[21] Y. Shiomi, S. Nakanishi, and T. Uehara, "Characteristics of two-phase flow in a channel formed by chevron type plates", *Exp. Therm. Fluid Sci*., vol. 28, no. 2-3, pp. 231-235, Jan. 2004. DOI: 10.1016/S0894-1777(03)00044-X.

[22] V. Grabenstein, A.E. Polzin, and S. Kabelac, "Experimental investigation of the flow pattern, pressure drop and void fraction of two-phase flow in the corrugated gap of a plate heat exchanger," *Int. J. Mutiph. Flow*, vol. 91, pp. 155-169, May 2017. DOI: 10.1016/j.ijmultiphaseflow.2017.01.012.

[23] D.H. Han, K.J. Lee, and Y.H. Kim, "The characteristics of condensation in brazed plate heat exchangers with different chevron angles," *J. Korean Phy. Soc*., vol. 43, no.1, pp. 66-73, Feb. 2003.

[24] A. Muller and S. Kabelac, "The experimental determination of heat transfer and pressure drop during condensation in a plate heat exchanger with corrugated plates," *WIT Trans. Eng. Sci*., vol. 83, pp. 337-349, Jul. 2014. DOI: 10.2495/HT140301.

[25] Y.Y. Yan, T.F. Lin, and B.C. Yang, "Evaporation heat transfer and pressure drop of refrigerant R134a in a plate heat exchanger", presented at the ASME ASIA '97 Congr., Singapore, Oct. 2, 1997.

[26] Y.H. Kim and G.J. Lee, "An experimental study on evaporation heat transfer and pressure drop in plated heat exchangers with different chevron angles," *Trans. Korean Soc. Mech. Eng*., Part B, vol. 26, no. 2, pp. 269-277, Feb. 2002. DOI: 10.3795/ksme-b.2002.26.2.269.

[27] D.H. Han, K.J. Lee, and Y.H. Kim, "Experiments on the characteristics of evaporation of R410A in brazed plate heat exchangers with different geometric configurations", *Appl. Therm. Eng*., vol. 23, no. 10, pp. 1209-1225, Jul. 2003. DOI: 10.1016/S1359-4311(03)00061-9.

[28] Y.Y. Hsieh and T.F. Lin, "Evaporation heat transfer and pressure drop of refrigerant R-410A flow in a vertical plate heat exchanger", *J. Heat Transf.*, vol. 125, no. 5, pp. 852-857, Oct. 2003. DOI: 10.1115/1.1518498.

[29] J.H. Park and Y.S. Kim, " Evaporation heat transfer and pressure drop characteristics of R-134a in the oblong shell and plate heat exchanger", *KSME Int. J.*, vol. 18, no. 12, pp. 2284-2293, 2004.

[30] F. Taboas, M. Valles, M. Bourouis, and A. Coronas, "Flow boiling heat transfer of ammonia/water mixture in a plate heat exchanger," *Int. J. Refrig.*, vol. 33, no. 4, pp. 695-705, Jun. 2010. DOI: 10.1016/j.ijrefrig.2009.12.005.

[31] M.S. Khan, T.S. Khan, M.C. Chyu, and Z.H. Ayub, "Experimental investigation of evaporation heat transfer and pressure drop of ammonia in a 30° chevron plate heat exchanger", *Int. J. Refrig.*, vol. 35, no. 6, pp. 1757-1765, Sep. 2012. DOI: 10.1016/j.ijrefrig.2012.05.019.

[32] T.S. Khan, M.S. Khan, M.C. Chyu, and Z.H. Ayub, "Experimental investigation of evaporation heat transfer and pressure drop in a 60° chevron plate heat exchanger", *Int. J. Refrig.*, vol. 35, no. 2, pp. 336-348, Mar. 2012. DOI: 10.1016/j.ijrefrig.2011.10.018.

[33] F. Vakili-Farahani, R.L. Amalfi, and J.R. Thome, "Two-phase flow and boiling of R245fa in a 1 mm pressing depth plate heat exchanger - Part I: Adiabatic pressure drop", *Interfacial Phenom. Heat Transf.*, vol. 2, no. 4, pp. 325-342, 2014. DOI: 10.1615/InterfacPhenomHeatTransfer.2015012027.

[34] E. Lee, H. Kang, and Y. Kim, "Flow boiling heat transfer and pressure drop of water in a plate heat exchanger with corrugated channels at low mass flux conditions," *Int. J. Heat Mass Transf.*, vol. 77, pp. 37-45, Oct. 2014. DOI: 10.1016/j.ijheatmasstransfer.2014.05.019.

[35] M.S. Khan, T.S. Khan, M.C. Chyu, and Z.H. Ayub, "Evaporation heat transfer and pressure drop of ammonia in a mixed configuration chevron plate heat exchanger," *Int. J. Refrig*., vol. 41, pp. 92-102, May 2014. DOI: 10.1016/j.ijrefrig.2013.12.015.

[36] T.S. Khan, M.S. Khan, M.C. Chyu, and Z.H. Ayub, "Ammonia evaporation in a mixed configuration chevron plate heat exchanger with and without miscible oil," *Int. J. Refrig*., vol. 51, pp. 120-134, Mar. 2015. DOI: 10.1016/j.ijrefrig.2014.12.002.

[37] R.L. Amalfi, J.R. Thome, V. Solotych, and J. Kim, "High resolution local heat transfer and pressure drop infrared measurements of two-phase flow of R245fa within a compact plate heat exchanger", *Int. J. Heat Mass Transf*., vol. 103, pp. 791-806, Dec. 2016. DOI: 10.1016/j.ijheatmasstransfer.2016.07.060.

[38] A. Desideri et al., "An experimental analysis of flow boiling and pressure drop in a brazed plate heat exchanger for organic Rankine cycle power systems," *Int. J. Heat Mass Transf*., vol. 113, pp. 6-21, Oct. 2017. DOI: 10.1016/j.ijheatmasstransfer.2017.05.063.

[39] J. Zhang et al., "Flow boiling heat transfer and pressure drop characteristics of R134a, R1234yf, and R1234ze in a plate heat exchanger for organic Rankine cycle units", *Int. J. Heat Mass Transf*., vol. 108, Part B, pp. 1787-1801, May 2017. DOI: 10.1016/j.ijheatmasstransfer.2017.01.026.

[40] D. Kim, D.C. Lee, D.S. Jang, Y. Jeon, and Y. Kim, "Comparative evaluation of flow boiling heat transfer characteristics of R-1234Ze(E) and R-134a in plate heat exchangers with different chevron angles", *Appl. Therm. Eng.*, vol. 132, pp. 719-729, Mar. 2018. DOI: 10.1016/j.applthermaleng.2018.01.019.

[41] D.C. Lee, D. Kim, S. Park, J. Lim, and Y. Kim, "Evaporation heat transfer coefficient and pressure drop of R-1233zd(E) in a brazed plate heat exchanger", *Appl. Therm. Eng*., vol. 130, pp. 1147-1155, Feb. 2018. DOI: 10.1016/j.applthermaleng.2017.11.088.

[42] D.C. Lee, D. Kim, W. Cho, and Y. Kim, "Evaporation heat transfer and pressure drop characteristics of R1234Ze(E)/R32 as a function of composition ratio in a brazed plate heat exchanger", *Int. J. Heat Mass Transf.*, vol. 140, pp. 216-226, Sep. 2019. DOI: 10.1016/j.ijheatmasstransfer.2019.06.004.

[43] K.S. Song, S. Yun, D.C Lee, K. Kim, and Y. Kim, "Evaporation heat transfer characteristics of R-245fa in a shell and plate heat exchanger for very-high-temperature heat pumps", *Int. J. Heat Mass Transf.*, vol. 151, article no. 119408, 10 pages, Apr. 2020. DOI: 10.1016/j.ijheatmasstransfer.2020.119408.

[44] J. Soontarapiromsook et al., "Experimental investigation on two-phase heat transfer of R134a during vaporization in a plate heat exchanger with rough surface", *Int. J. Heat Mass Transf.*, vol. 160, article 120221, 10 pages, Oct. 2020. DOI: 10.1016/j.ijheatmasstransfer.2020.120221.

[45] C.U. Jo, D.C. Lee, H.J. Chung, Y. Kang, and Y. Kim, "Comparative evaluation of the evaporation heat transfer characteristics of a low-GWP-refrigerant R-1234Ze(E) between shell-and-plate and plate heat exchangers", *Int. J. Heat Mass Transf.*, vol. 153, article no. 119598, 10 pages, Jun. 2020. DOI: 10.1016/j.ijheatmasstransfer.2020.119598.

[46] J. Zhang and F. Haglind, "Experimental analysis of high temperature flow boiling heat transfer and pressure drop in a plate heat exchanger", *Appl. Therm. Eng.*, vol. 196, article no. 117269, 14 pages, Sep. 2021. DOI: 10.1016/j.applthermaleng.2021.117269.

[47] J. Yang, D.C. Lee, and Y. Kim, "Experimental study on evaporation heat transfer characteristics of R32 in a plate heat exchanger", paper no. ICMFHT 106, presented at the 6th World Congr. on Momentum, Heat and Mass Transfer, Lisbon, Portugal, Jun. 17-19, 2021. DOI: 10.11159/icmfht21.lx.106.

[48] X. Huang, J. Zhang, and F. Haglind, "Experimental analysis of high temperature flow boiling of zeotropic mixture R134a/R245fa in a plate heat exchanger", *Appl. Therm. Eng*., vol. 220, article no. 119652, 13 pages, Feb. 2023. DOI: 10.1016/j.applthermaleng.2022.119652.

[49] F. Taboas, M. Valles, M. Bourouis and A. Coronas, "Assessment of boiling heat transfer and pressure drop correlations of ammonia/water mixture in a plate heat exchanger," *Int. J. Refrig*., vol. 35, no. 3, pp. 633-644, May 2012. DOI: 10.1016/j.ijrefrig.2011.10.003.

[50] R.W. Lockhart and R.C. Martinelli, "Proposed correlation of data for two-phase, two-component flow in pipes," *Chem. Eng. Prog*., vol. 45, no. 1, 1949, pp. 39-48.

[51] K. Nilpueng and S. Wongwises, "Two-phase gas-liquid flow characteristics inside a plate heat exchanger," *Exp. Therm Fluid Sci*., vol. 34, no. 8, pp. 1217-1229, Nov. 2010. DOI: 10.1016/j.expthermflusci.2010.05.001.

[52] G.A. Longo, S. Mancin, G. Righetti, and C. Zilio, "Boiling of the new low-GWP refrigerants R1234Ze(Z) and R1233Zd(E) inside a small commercial brazed plate heat exchanger", *Int. J. Refrig*., vol. 104, pp. 376-385, Aug. 2019. DOI: 10.1016/j.ijrefrig.2019.05.034.

[53] L.F. Moody, “Friction factors for pipe flow,” *Trans. ASME*, vol. 66, pp. 671-678, Nov. 1944.

[54] G.K. Filonenko, “Hydraulic resistance in pipes,” *Teploenergetica*, vol. 4, no. 4, pp. 40-54, 1954.

Table 1 Condensation pressure drop data in plate heat exchangers

Study	Fluid and Parameters	No. of data		% Of Data	Experimental uncertainty (ΔP)
		Laminar	Turbulent		
Yan et al. [2] 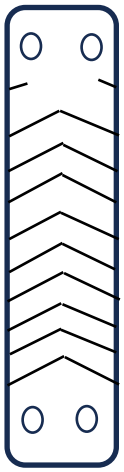	R134a, d_h = 6.6 mm, β = 60°, Z_P = 450 mm, A_P = 315 cm^2, q" = 10-16 kW/m^2s, T_{sat} = 26.71-35.53°C, G = 6-120 kg/m^2s, x = 0.1-0.9.	79	16	6.5%	±20%
Kuo et al. [3] 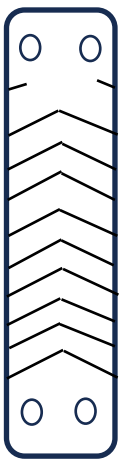	R410A, d_h = 10-20 mm, β = 60°, Z_P = 450 mm, A_P = 315 cm^2, q" = 10-20 kW/m^2 T_{sat} = 19.81°C, G = 50-150 kg/m^2s.	51	51	7%	±16.5%
Djordjevic et al. [4]	R134a, d_h = 3.2 mm, β =	25	0	1.71%	±20%

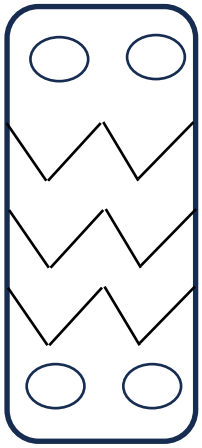	63.26°, Z_P = 872 mm, A_P = 0.42 m^2, q" = 11.5-17.1 kW/m^2, T_{sat} = 27.5°C, G = 35-65 kg/m^2s.				
Shon et al. [5] 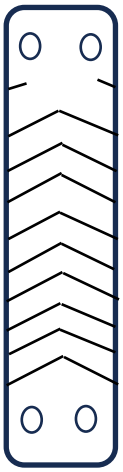	R1233zd(E), d_h = 3.32 mm, β = 60°, Z_P = 234 mm, A_P = 147.4 cm^2, q" = 2.5-4.5 kW/m^2s, T_{sat} = 37.68°C, G = 13-23.8 kg/m^2s.	102	0	7%	1.5%
Soontarapiromsook et al. [6] 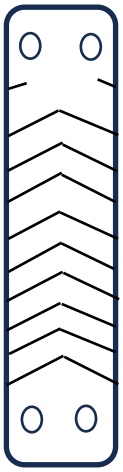	R134a, d_h = 5 mm, β = 65°C, Z_P = 360 mm, A_P = 320 cm^2, q" = 5-15 kg/m^2s, T_{sat} = 40°C and 50°C, G = 61-89 kg/m^2s.	30	2	2.1%	±8.41%

Zhang et al. [7] 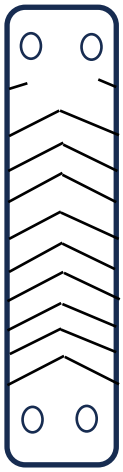	R134a, R1234ze(E), R245fa, d_h = 3.4 mm, β = 65°C, Z_P = 317 mm, A_P = 240.9 cm^2, q" = 0 kW/m^2s, T_{sat} = 30-60°C, G = 53 kg/m^2s.	174	0	11.9%	3.2% to 15.2%
Kwon et al. [8] 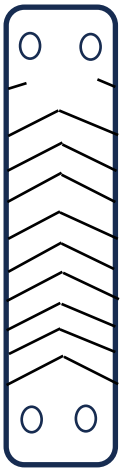	R1233zd(E), d_h = 3.88 mm, β = 60°, Z_P = 872 mm, A_P = 0.42 m^2, q" = 2.5-4.5 kW/m^2s, T_{sat} = 37.78°C and 44.72°C, G = 13-23.8 kg/m^2s.	97	0	6.7%	15.96%
Park and Kim [9] 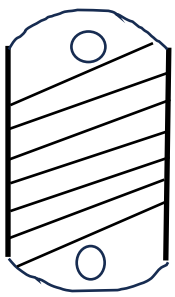	R134a, d_h = 4-8 mm, β = 45°, Z_P = 361 mm, A_P = 600.4 cm^2, q" = 4-8	87	2	6.1%	Not available

	kW/m^{2}s, T_{sat} = 30-40°C, G = 40-80 kg/m^{2}s.				
Park et al. [10] 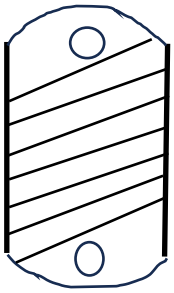 (Oblong shell and plate PHE)	R410A, d_h = 5.6 mm, β = 45°, Z_P = 361 mm, A_P = 600.4 cm^2, q" = 4-8 kW/m^{2}s, T_{sat} = 30°C and 40°C, G = 40-80 kg/m^{2}s.	59	30	6.1%	Not available
Tao et al. [11] 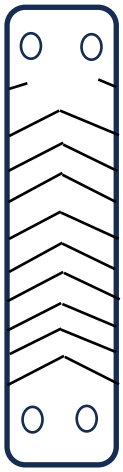	NH_3, d_h = 2.99 mm, β = 63°C, Z_P = 668 mm, A_P = 0.64 m^2, q" = 0 kW/m^{2}s, T_{sat} = 13.4-22.6°C, G = 21-71 kg/m^{2}s.	69	0	4.7%	±14.2%
Tao and Ferreira [12] 	NH_3, d_h = 2.99 mm, β = 63°C, q" = 0 kW/m^2, Z_P = 668 mm, A_P = 0.64 m^2	31	0	2.1%	±14.2%

	T_{sat} = 13.37°C, G = 30-71 kg/m^{2}s.				
Ko et al. [13] 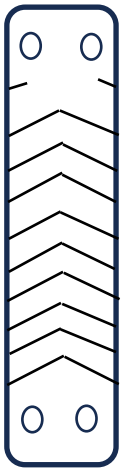	R124, d_h = 3.32 mm, β = 30-60°C, Z_P = 287 mm, A_P = 335.79 cm^2, q" = 2.5-4.5 kW/m^2, T_{sat} = 37.74-50.73°C, G = 19.9-26 kg/m^{2}s.	90	0	6.2%	3.57%
Jung et al. [14] 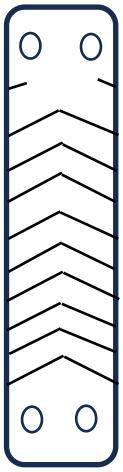	R124, d_h = 3.88 mm, β = 30° and 60°, Z_P =234 mm, A_P = 240 cm^2, q" = 2.5-3.5 kW/m^{2}s, T_{sat} = 47.17°C and 52.18°C, G = 2.5-26.5 kg/m^{2}s.	96	0	6.6%	3.14%

Kwon et al. [15] 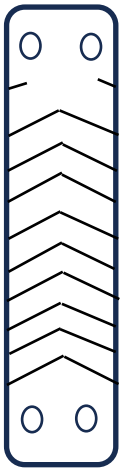	R1233zd(E), d_h = 4.2 mm, β = 60°, Z_P =234 mm, A_P = 240 cm^2, q" = 1.5-2.5 kW/m^2s, T_{sat} = 44.72-56.07°C, G = 10 kg/m^2s and 13 kg/m^2s.	46	0	3.2%	2.97%
Lee et al. [16] 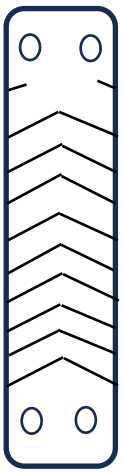	R1234ze(E), d_h = 3.88 mm, Z_P = 245 mm, A_P = 183.75 cm^2, β = 60°, q" = 0 kW/m^2s, T_{sat} = 15°C, G = 50-130 kg/m^2s.	39	0	2.7%	±7.97%
Wang et al. [17] 	R365mfc, d_h = 5.195 mm, β = 45°, Z_P = 380 mm, A_P = .144 m^2, q" = 0 kW/m^2s, T_{sat} =	16	0	1.1%	±17.8%

	43°C, G = 17.05-44.74°C.				
Hu and Ma [18] 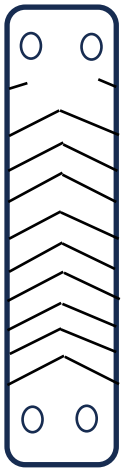	Steam and water-ethanol mixture, d_h = 6 mm, β = 60°, Z_P = 285 mm, A_P = 200 cm^2, q" = 0 kW/m^2s, T_{sat} = 87.17-127.29°C, G = 5.9-14.9 kg/m^2s.	245	0	16.8%	±6.64%

Table 2 Comparative analysis of the condensation pressure drop database [2-18]

Study	Fluid	Refrigerant properties					MBD	RMSD
		T_{sat} °C	ρ_L (Kg/m^3)	ρ_V (Kg/m^3)	P_r	T_r		
Yan et al. [2]	R134a	26.7-35.3	1165.3-1200.2	34.1-44.1	0.17-0.22	0.26-0.35	-30.6%	75.4%
Kuo et al. [3]	R410A	19.81	1073.2	59.65	0.32	0.28	-32.1%	138.6%
Djordjevic et al. [4]	R134a	27.5	1197.2	34.9	0.18	0.27	-260.2%	685.7%
Shon et al. [5]	R1233zd(E)	37.7	1224.8	11.9	0.06	0.23	-20.4%	6.5%
Soontarapiromsook et al. [6]	R134a	40, 50	1102.3, 1146.7	50.1, 66.3	0.25, 0.32	0.4, 0.5	-14.8%	6.8%
Zhang et al. [7]	R134a, R1234ze(E), R245fa	30-60	1125.3 1102.5 1248.6	59.1 44.1 23.8	0.29 0.2 0.1	0.44 0.49 0.55	5.2%	27.6%
Kwon et al. [8]	R1233zd(E)	37.8, 44.7	1197.7, 1231.5	10.9, 16	0.06, 0.08	0.23, 0.27	-31.4%	17.5%
Park and Kim [9]	R134a	30-40	1146.7-1187.5	37.5-50.1	0.19-0.25	0.3-0.4	-9%	3.6%
Park et al. [10]	R410A	30, 40	975.3, 1032.7	75.3, 101.7	0.39, 0.5	0.43, 0.57	-35.1%	85.1%
Tao et al. [11]	NH_3	13.4-22.6	606.4-619.8	5.4-7.3	0.06-0.08	0.1-0.17	-9.2%	44.6%
Tao and Ferreira [12]	NH_3	13.4	619.8	5.43	0.06	0.1	1.5%	4.1%
Ko et al. [13]	R124	37.7-50.7	1260.2-1310	34.2-48.8	0.15-0.22	0.31-0.41	-1.8%	14.2%

Jung et al. [14]	R124	47.2, 52.8	1235.6, 1274.3	44.4, 57.2	0.2, 0.25	0.39, 0.43	7.1%	24.4%
Kwon et al. [15]	R1233zd(E)	44.7-56.1	1183.5-1213.5	13.4-18.6	0.08-0.1	0.27-0.34	66.1%	67.8%
Lee et al. [16]	R1234ze(E)	15	1195	19.3	0.1	0.14	48.9%	58.5%
Wang et al. [17]	R365mfc	43	1217.7	6.6	0.03	0.23	-76.4%	101.9%
Hu and Ma [18]	Water-Ethanol mixture Steam	87.2-127.3 102.3	924.4-959.1 956.7	0.53-1.49 0.65	0.004-0.006 0.005	0.23-0.34 0.27	-10%	46.4%

Table 3 Sensitivity analysis of Eq. (5) with variations in one parameter [6] and others constant

Parameter	Variation	ϕ_{LO}^2 (Eq. (5))	% Difference
Re_{LO} (Nominal =1682)	0%	1499.97	0%
	+10%	1623.91	8.3%
	-10%	1373.94	-8.4%
$\frac{\rho_L}{\rho_V}$ (Nominal = 22.9)	0%	1499.97	0%
	+10%	1740.02	16%
	-10%	1272.48	-15.2%
X (Nominal = 0.3516)	0%	1499.97	0%
	+10%	1538.53	2.6%
	-10%	1458.51	-2.8%
P_r (Nominal = 0.2505)	0%	1499.97	0%
	+10%	1493.55	-0.43%
	-10%	1507.1	+0.48%
We (Nominal = 0.00265)	0%	1499.97	0%
	+10%	1394.89	-7%
	-10%	1625.36	+8.4%
x (Nominal = 0.11)	0%	1499.97	0%
	+10%	1512.76	0.85%
	-10%	1484.44	-1%
β* (Nominal = 1.134)	0%	1499.97	0%
	+10%	1570.94	4.73%
	-10%	1425.25	-4.98%
	0%	1499.97	0%

$\frac{\mu_L}{\mu_V}$ (Nominal = 13.05)	+10%	1468	-2.13%
	-10%	1536.11	2.41%
Bd (Nominal = 0.04398)	0%	1499.97	0%
	+10%	1607.67	+7.2%
	-10%	1389.16	-7.4%
T_r (Nominal = 0.396)	0%	1499.97	0%
	+10%	1559.44	3.96%
	-10%	1436.85	-4.2%

Table 4 Predictive correlations for condensation in plate heat exchangers

Study	Fit
Equation (5) ϕ_{LO}^2 $= 0.12Re_{LO}^{0.83}\left(\frac{\rho_L}{\rho_V}\right)^{0.0.036} X^{0.27}P_r^{-0.045}We^{-0.76}x^{0.047}\beta^{*0.49}\left(\frac{\mu_L}{\mu_V}\right)^{0.61} Bd^{0.73}T_r^{0.41}$ (Re_{LO} = 13-7105, 0 < x < 1, P_{sat} = 0.9-24.26 bar, q" = 0-20 kW/m^2, G = 2.5-150 kg/m^{2}s, d_h = 2.99-6.6 mm, β = 30-65°, P_r = 0.004-0.504)	MBD = -13.9% RMSD = 66.5% R^2 = 0.73 Fit: 21.4% in ±10%, 54.1% in ±30%, and 72.3% in ±50%
Wang et al. [19] $\phi_L^2 = 0.60959 + 0.03904lnX + \frac{1.44957}{X}$ Air-water mixture, T_{sat} = 20°C, Re_{eq} = 100-900, G = 25-100 kg/m^{2}s, no phase change.	MBD = 82.4% RMSD = 119.6% R^2 = 0 Fit: 0% in ±50%
Jiang and Bai [20] $\phi_L^2 = 1 + \frac{5.3 + 0.0004Re_{mix}}{X} + \frac{0.3}{X^2}$ $Re_{mix} = \frac{(G_L + G_V)d_h}{(1-x)\mu_L + x\mu_V};\ G_L = (1-x)G, G_V = Gx$ Air-water mixture, T_{sat} = 20°C, Re_{mix} = 1000-7000, no phase change.	MBD = -1542% RMSD = 9478% R^2 = 0 Fit: 0% in ±50%
Shiomi et al. [21] $\phi_L^2 = 1 + \frac{8}{X} + \frac{1}{X^2}$ Air-water mixture, T_{sat} = 20°C, Re_L = 44-2400, Re_V = 44-340, G_L = 0.012 kg/s, no phase change.	MBD = -5161% RMSD = 30,563% R^2 = 0 Fit: 0% in ±50%
Grabenstein et al. [22]	MBD = 68.8%

$\phi_L = 1 + \frac{2.57}{X}$ Air-water mixture, R365mfc, T_{sat} = 20°C, Re_{TP} = 5000-40,000, G_L = 1-1000 kg/m^{2}s, x = 0-1	RMSD = 168.5% R^2 = 0 Fit: 0% in ±50%

Table 5 Condensation heat transfer data for evaluation

Study	Fluid	No. of data		% Of Data	Experimental uncertainty (ΔP)	Fit
		Laminar	Turbulent			
Kwon et al. [15] 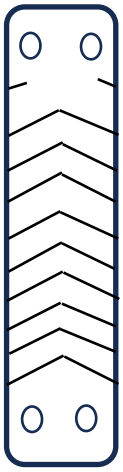	R1233zd(E), d_h = 4.2 mm, β = 60°, Z_P =234 mm, A_P = 240 cm^2, q" = 1.5-2.5 kW/m^2s, T_{sat} = 44.72-56.07°C, G = 10 kg/m^2s and 13 kg/m^2s.	46	0	62.3%	2.85%	MBD = -4.1% RMSD = 41.1%
Han et al. [23] 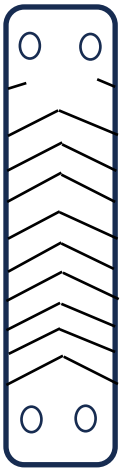	R410A, d_h = 5.1 mm, β = 20-45°, Z_P = 476 mm, A_P = 328.4 cm^2, q" = 5 kW/m^2, T_{sat} = 20°C and 30°C, G = 34 kg/m^2s.	14	0	18.2%	±6.89% (±250 Pa)	MBD = 13.7% RMSD = 23.6%

Muller and Kabelac [24] 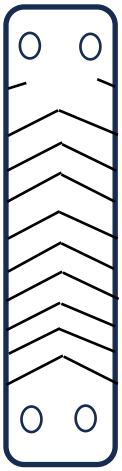	R134a and steam, d_h = 5.194 mm, β = 27° and 63°, Z_P = 936 mm, A_P = 0.36 m^2, T_{sat} = 25.9°C and 112.3°C, G = 11.1-55.9 kg/m^2s.	7	0	19.5%	Not available	MBD = 11.1% RMSD = 25.9%

Table 6 Evaporation heat transfer data [25-48] in plate heat exchangers

Study	Fluid and Test Parameters	No. of data		% Of Data	Experimental uncertainty (ΔP)
		Laminar	Turbulent		
Yan et al. [25] 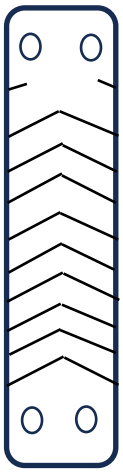	R134a, d_h = 6 mm, β = 60°, Z_P = 450 mm, A_P = 315 cm^2, T_{sat} = 25.48°C, q" = 11-15 kW/m^2, G = 55 kg/m^2s and 70 kg/m^2s, x = 0.1-0.9.	38	4	2.2%	±3.33% (±800 Pa)
Kim and Lee [26] 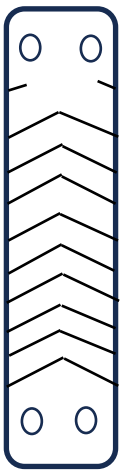	R22 and R410A, d_h = 4.3 mm, β = 20-45°, Z_P = 476 mm, A_P = 328 cm^2, q" = 5.5 kW/m^2, T_{sat} = 5-15°C, G = 27 kg/m^2s, x = 0.2-0.95.	68	0	3.61%	±2.63% (±250 Pa)

Han et al. [27] 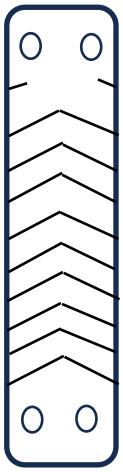	R410A, d_h = 4.3 mm, β = 20-45°, Z_P = 476 mm, A_P = 328 cm^2, q" = 10-20 kW/m^2, T_{sat} = 5-15°C, G = 27 kg/m^2s, x = 0.2-0.95.	52	0	2.76%	±2.5% (±250 Pa)
Hsieh and Lin [28] 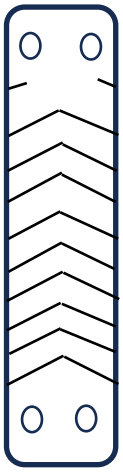	R410A, d_h = 6.6 mm, β = 60°, Z_P = 450 mm, A_P = 315 mm, q" = 4-6 kW/m^2, T_{sat} = 9.7°C and 14.7°C, G = 50-100 kg/m^2s, x = 0.1-0.9.	11	46	3.02%	±1.5%
Park and Kim [29] 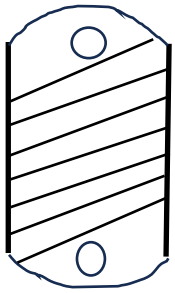	R134a, d_h = 5.6 mm, β = 45°, Z_P = 316 mm, A_P = 600.4 cm^2, q" = 6 kW/m^2, T_{sat} =	91	0	4.83%	Not available

(Oblong shell-plate PHE)	0.01-10°C, G = 40-80 kg/m^{2}s, x = 0.1-0.9.				
Taboas et al. [30] 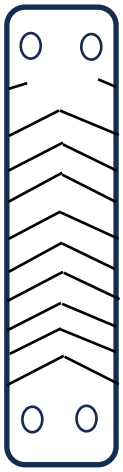	Ammonia-water mixture, d_h = 5.6 mm, β = 45°, Z_P = 466 mm, A_P = 521.9 cm^2, q" = 35 kW/m^2, T_{sat} = 133.8°C, G = 140 kg/m^{2}s, x = 0.04-0.2.	0	12	0.63%	±18.2%
Khan et al. [31] 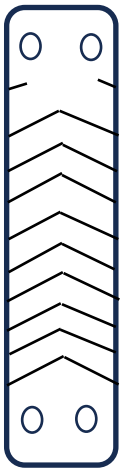	NH_3, d_h = 4.4 mm, β = 30°C, Z_P = 565 mm, A_P = 950 cm^2, q" = 32.5 kW/m^2, T_{sat} = -2°C to -25°C, G = 5.5 kg/m^{2}s, x = 0.2-0.4.	35	0	1.86%	±3.0%
Khan et al. [32]	NH_3, d_h = 4.4 mm, β = 60°, Z_P = 565 mm,	53	0	2.81%	±2.6%

	A_P = 950 cm^2, q” = 7-49 kW/m^2, T_{sat} = -2°C to -25°C, G = 5.5 kg/m^2s, x = 0.2-0.5.				
Vakili-Farahani et al. [33] 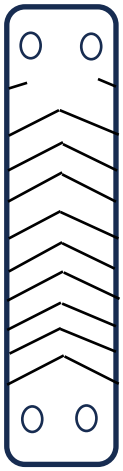	R245fa, d_h = 1.7 mm, β = 65°, Z_P = 228 mm, A_P = 114 cm^2, q” = 0 kW/m^2, T_{sat} = 25-35°C, G = 10-40 kg/m^2s, x = 0.01-0.7.	46	0	2.44%	15%
Lee et al. [34] 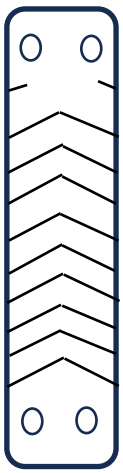	Water, d_h = 5 mm, β = 60°, Z_P = 357 mm, A_P = 214.2 mm, q” = 15-30 kW/m^2. T_{sat} = 103.93°C, G = 14.5-24 kg/m^2s, x = 0.1-0.6.	69	0	3.66%	±1.2%

Khan et al. [35] 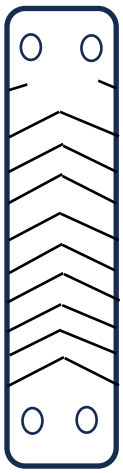	NH_3, d_h = 5.8 mm, β = 45°C, Z_P = 565 mm, A_P = 950 cm^2, q" = 21.2-49.1 kW/m^2, T_{sat} = -2°C to -25°C, G = 6.5 kg/m^2s, x = 0.5-0.8.	30	0	1.59%	±2.8%
Khan et al. [36] 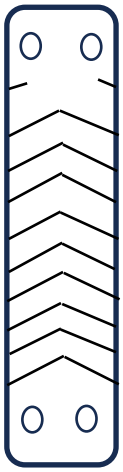	NH_3, d_h = 5.8 mm, β = 45°C, Z_P = 565 mm, A_P = 950 cm^2, q" = 21.2-49.1 kW/m^2, T_{sat} = -2°C and -25°C, G = 6.5 kg/m^2s, x = 0.5-0.75.	10	0	0.53%	±3%
Amalfi et al. [37] 	R245fa, d_h = 1.7 mm, β = 65°, Z_P = 228 mm, A_P = 200 cm^2, q" = 0 kW/m^2, T_{sat} = 25-30.5°C, G =	48	0	2.55%	±2.4%

	15-45 kg/m^{2}s, x = 0.1-0.7.				
Desideri et al. [38] 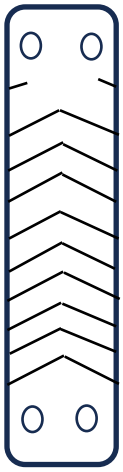	R245fa and R1233zd(E), d_h = 3.4 mm, β = 65°, Z_P = 278 mm, A_P = 232.9 cm^2, q" = 0 kW/m^2, T_{sat} = 100-130°C, G = 80 kg/m^{2}s and 100 kg/m^{2}s, x = 0.3-0.7.	54	0	2.86%	±11.6%
Zhang et al. [39] 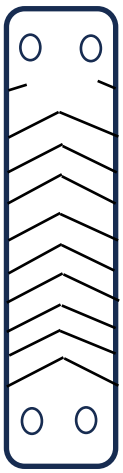	R134a, R1234ze, and R1234yf, d_h = 3.4 mm, β = 65°, Z_P = 278 mm, A_P = 111.2 cm^2, q" = 0 kW/m^2, T_{sat} = 60-80°C, G = 86-137 kg/m^{2}s, x = 0.5-0.99.	248	16	14%	15.6%

Kim et al. [40] 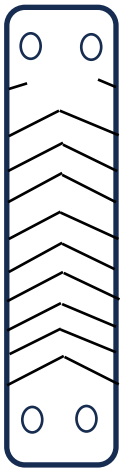	R1234ze(E), d_h = 3.37 mm, β = 30° and 60°, Z_P = 234 mm, A_P = 273.8 cm^2, q" = 6.5-10 kW/m^2, T_{sat} = 5-15°C, G = 21.3-58.1 kg/m^2s, x = 0.1-0.9.	91	0	4.83%	±3.91%
Lee et al. [41] 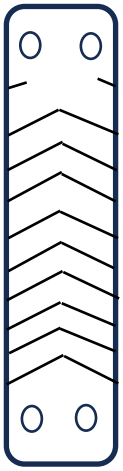	R1233zd(E) and R245fa, d_h = 3.88 mm, β = 60°, Z_P = 234 mm, A_P = 147.4 cm^2, q" = 6.5 kW/m^2, T_{sat} = 60-80°C, G = 32-58 kg/m^2s, x = 0.1-0.9.	43	0	2.28%	±5.19%
Lee et al. [42]	R1234ze(E), R32, and R134a, d_h = 3.88 mm, β =	37	0	1.96%	±5.31%

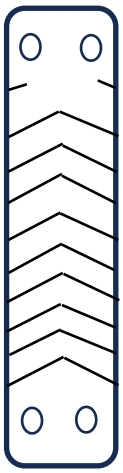	60°, Z_P = 234 mm, A_P = 147.4 cm^2, q" = 6.45 kW/m^2, T_{sat} = 15°C, G = 32-58 kg/m^2s, x = 0.1-0.9.				
Song et al. [43] 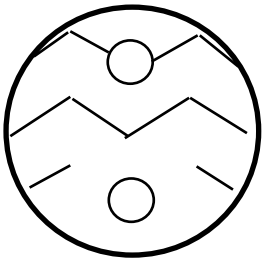 (Shell-plate HX)	R245fa, d_h = 5 mm and 6 mm, β = 50°, Z_P = 227 mm, A_P = 0.34 m^2, q" = 6-7.5 kW/m^2, T_{sat} = 60-80°C, G = 15-32 kg/m^2s, x = 0.2-0.8.	53	0	2.81%	±6.28%
Soontarapiromsook et al. [44] 	R134a, d_h = 5-15 mm, β = 65°, Z_P = 360 mm, A_P = 320 cm^2, q" = 10 kW/m^2, T_{sat} = 20°C, G = 67-	20	0	1.06%	±8.23%

	96 kg/m^{2}s, x = 0.1-0.8.				
Jo et al. [45] 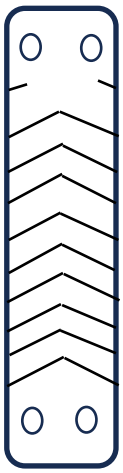	R1234ze(E), d_h = 3.315 mm, β = 60°, Z_P = 287 mm, A_P = 335.8 cm^2, q" = 2.8-6.9 kWm^2, T_{sat} = 15°C, G = 20-45 kg/m^{2}s, x = 0.2-0.8.	35	0	1.86%	±2.2%
Zhang and Haglind [46] 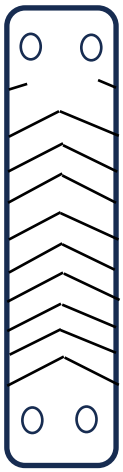	R134a, R1234ze(E), R236fa, R245fa, R1233zd(E), Propane, Isobutane, d_h = 3.4 mm, β = 65°, Z_P = 278 mm, A_P = 111.2 cm^2, q" = 0 kW/m^2, T_{sat} = -50.3°C to	126	189	16.71%	18.2%

	145.1°C, G = 52-137 kg/m^{2}s, x = 0.1-0.5.				
Yang et al. [47] 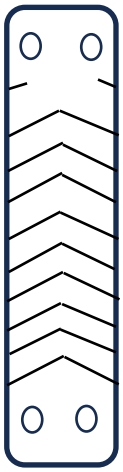	R32 and R410A, d_h = 3.88 mm, β = 60°, Z_P = 234 mm, A_P = 147.4 cm^2, q" = 6.45 kW/m^2, T_{sat} = 5°C, G = 50-90 kg/m^{2}s, x = 0.1-0.9.	29	1	1.59%	Not available
Huang et al. [48] 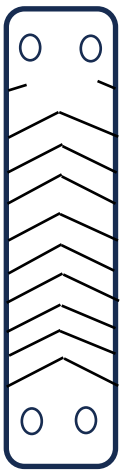	R134a and R245fa mixture, d_h = 2 mm, β = 65°, Z_P = 278 mm, A_P = 111.2 cm^2, q" = 27 kW/m^2, T_{sat} = 67.4-111.5°C, G = 103-137 kg/m^{2}s, x = 0.3-0.8.	325	0	17.24%	18.6%

Table 7 Comparative analysis of the evaporation pressure drop database [25-48]

Study	Fluid	Refrigerant properties					MBD	RMSD
		T_{sat} °C	ρ_L (Kg/m^3)	ρ_v (Kg/m^3)	P_r	T_r		
Yan et al. [25]	R134a	25.5-31.3	1182.2-1204.8	32.8-39	0.17-0.2	0.8-0.81	52%	52.8%
Kim and Lee [26]	R410A R22	5-15 15	1106-1149.6 1228.6	35.2-48 33.4	0.19-0.26 0.16	0.81-0.84 0.78	50%	55%
Han et al. [27]	R410A	5-15	1106-1150	35-48	0.19-0.26	0.81-0.84	10%	38.4%
Hsieh and Lin [28]	R410A	9.7, 14.8	1107.3, 1129.5	40.9, 47.8	0.22, 0.26	0.82, 0.84	-196%	239.4%
Park and Kim [29]	R134a	0.01-10	1261-1295	14.4-20.3	0.07-0.1	0.73-0.76	-9%	34.9%
Taboas et al. [30]	NH_3	133.8	783.6	4.4	0.04	0.75	19%	31.6%
Khan et al. [31]	NH_3	-25 to -2	641.3 – 664.5	1.3-3.2	0.01-0.04	0.45-0.5	-46%	61.1%
Khan et al. [32]	NH_3	-25 to -2	641.3 – 664.5	1.3-3.2	0.01-0.04	0.45-0.5	17%	22.7%
Vakili-Farahani et al. [33]	R245fa	25-35	1311-1338.5	8.6-12.02	0.04-0.06	0.7-0.72	18%	26.8%
Lee et al. [34]	Water	103.9	955.5	0.68	0.005	058	14%	43.6%
Khan et al. [35]	NH_3	-25 to -2	641.3-671.5	1.3-3.2	0.01-0.04	0.61-0.67	-157%	176%

Khan et al. [36]	NH_3	-2, -25	641.3, 671.5	3.2, 1.3	0.01, 0.035	0.67, 0.61	-153%	175%
Amalfi et al. [37]	R245fa	25-30.5	1323-1329	8.6-10.3	0.04-0.05	0.7-0.71	28%	34.3%
Desideri et al. [38]	R245fa R1233zd(E)	100-130 100-130	940-1093 927-1050	72.8-155.3 14.3-113.5	0.29-0.48 0.39-0.53	0.87-0.94 0.91-0.94	-12%	35.9%
Zhang et al. [39]	R134a R1234ze R1234yf	60-80 60-80 60-80	928-1052 933-1033 809-941	87-155 70-120 100-180	0.41-0.65 0.46 0.5	0.89-0.94 0.89-0.94 0.89-0.92	1%	58.1%
Kim et al. [40]	R1234ze(E)	5-15	1195-1225	13.9-19.3	0.095-0.1	0.66-0.68	-62%	108.6%
Lee et al. [41]	R1233zd(E) R245fa	60-80 60-80	1115-1173 1170-1237	20.7-34.8 25.7-44	0.11-0.14 0.13-0.22	0.78-0.8 0.8-0.83	-20%	43%
Lee et al. [42]	R1234ze(E)/ R32 mixture R32	15 15	1031-1195 1000.9	23.3-32.7 35.2	0.21-0.27 0.2	0.68 0.82	56%	57%

	R134a	15	1243.4	23.8	0.28	0.77		
Song et al. [43]	R245fa	60-80	1170-1234	25.7-44	0.13-0.21	0.78-0.83	49%	60%
Soontarapiromsook et al. [44]	R134a	20	1225.3	27.8	0.14	0.8	23%	30.6%
Jo et al. [45]	R1234ze(E)	15	1195	19.3	0.1	0.68	-22%	31.7%
Zhang and Haglind [46]	R134a R1234ze(E) R236fa R245fa R1233zd(E) Propane Isobutane	81 87.8 70.7 122 142 73.4 -43.5	927.6 883.5 990.4 987.7 864 394.2 628	155.5 150 170.1 126.1 151.3 69.99 0.74	0.65 0.65 0.65 0.55 0.65 0.65 0.65	0.94 0.85 0.86 0.99 0.94 0.94 0.56	-36%	101%
Yang et al. [47]	R32 R410A	5 5	1038 1150	25.9 35.2	0.16 0.2	0.79 0.81	13%	30.6%
Huang et al. [48]	R134a/R245fa mixture	112	951	121.1	0.57	0.93	-3%	33%

Table 8 Sensitivity analysis of Eq. (6) with one parameter [48] variation and others constant

Parameter	Variation	ϕ_{LO}^2 (Eq. (6))	% Difference
Re_{LO} (Nominal = 1130)	0%	117.59	0%
	+10%	127.15	+8.1%
	-10%	107.85	-8.2%
Co (Nominal = 0.516)	0%	117.59	0%
	+10%	114.93	-2.3%
	-10%	120.6	+2.6%
Bo (Nominal = 0.00244)	0%	117.59	0%
	+10%	117.81	+0.19%
	-10%	117.35	-0.2%
X (Nominal = 0.7785)	0%	117.59	0%
	+10%	120.51	+2.5%
	-10%	114.43	-2.7%
P_r (Nominal = 0.55)	0%	117.59	0%
	+10%	113.94	-3.1%
	-10%	121.76	+3.5%
Bd (Nominal = 14.08)	0%	117.59	0%
	+10%	123.33	+4.9%
	-10%	111.55	-5.1%
We (Nominal = 9.65)	0%	117.59	0%
	+10%	111.56	-5.1%
	-10%	124.63	+5.98%
	0%	117.59	0%

β^* (Nominal = 1.134)	+10%	115.48	-1.8%
	-10%	119.96	+1.71%
T_r (Nominal = 0.925)	0%	117.59	0%
	+10%	127.93	+8.8%
	-10%	107.13	-8.9%
$\frac{\rho_L}{\rho_V}$ (Nominal = 7.84)	0%	117.59	0%
	+10%	117.08	-0.4%
	-10%	118.15	+0.47%
$\frac{\mu_L}{\mu_V}$ (Nominal = 7.53)	0%	117.59	0%
	+10%	122.58	+4.2%
	-10%	112.3	-4.5%

Table 9 Predictive correlations for evaporation in plate heat exchangers

Study	Fit
Equation (6) $\phi_{LO}^2 = 0.14 Re_{LO}^{0.82} Co^{-0.24} Bo^{0.02} X^{0.26} P_r^{-0.33} Bd^{0.5} We^{-0.55} \beta^{*-0.19} T_r^{0.88} \left(\frac{\rho_L}{\rho_V}\right)^{-0.05} \left(\frac{\mu_L}{\mu_V}\right)^{0.44}$ (Re_{LO} = 19-4870, P_{sat} = 0.165-27.63 bar, q" = 0-49.1 kW/m^2, G = 5.5-140 kg/m^{2}s, 0 < x < 1, d_h = 1.7-15 mm, β = 20-65°, P_r = 0.005-0.65)	MBD = -10.1% RMSD = 73.5% R^2 = 0.79 15.5% in ±10%, 49.3% in ±30%, and 71.2% in ±50%
Vakili-Farahani et al. [33] $\phi_L^2 = 1 + \frac{14.14}{X_{turb,turb}} + \frac{1}{X_{turb,turb}^2}$ (R245fa, Re_{LO} = 21-178, x = 0.02-8, T_{sat} = 19-35°C, G = 10-40 kg/m^{2}s, x = 0.02-0.8)	MBD = -505.6% RMSD = 8579% R^2 = 0 2.5% in ±10%, 8.5% in ±30%, 21% in ±50%
Taboas et al. [49] $\phi_L^2 = 1 + \frac{3}{X_{turb,turb}} + \frac{1}{X_{turb,turb}^2}$ (Ammonia-water mixture, Re_{eq} = 1500-8000, P_{sat} = 7-15 bar, G = 70-140 kg/m^{2}s, q" = 20-50 kW/m^2, x < 0.22)	MBD = -399.3% RMSD = 7850% R^2 = 0 1.5% in ±10%, 3.9% in ±30%, 7.4% in ±50%

Lockhart and Martinelli [50] $\phi_L^2 = 1 + \frac{C}{X_{turb,turb}} + \frac{1}{X_{turb,turb}^2}$ C = 12 (Re_{LO} < 2000 and Re_v > 2000) C = 10 (Re_{LO} > 2000 and Re_v < 1000) C = 5 (Re_{LO} < 1000 and Re_v < 1000) (oil-air, water-air, benzene-air, and kerosene-air mixtures, T_{sat} = 10-32°C, Re_L = 1-124,000, no phase change)	MBD = -36,050% RMSD = 168,698% R^2 = 0 0.75% in ±10%, 1.8% in ±30%, 4.3% in ±50%
Nilpueng and Wongwises [51] $\phi_L^2 = 1.339 + \frac{4.492}{X}$ (air-water mixture, Re_L = 0.2-19, T_{sat} = 20°C, G = 50-3800 kg/m^{2}s)	MBD = - 268.7% RMSD = 1117% R^2 = 0 0.2% in ±10%, 0.9% in ±30%, 2.1% in ±50%

Table 10 Evaporation heat transfer data for evaluation

Study	Fluid and Test Parameters	No. of data		% Of Data	Experimental uncertainty (ΔP)	Fit
		Laminar	Turbulent			
Amalfi et al. [37] 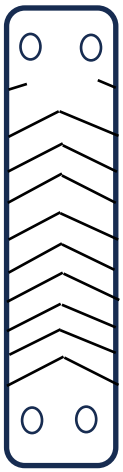	R245fa, , d_h = 1.7 mm, β = 65°, Z_P = 228 mm, A_P = 200 cm^2, q" = 0 kW/m^2, T_{sat} = 25-30.5°C, G = 15-45 kg/m^2s, x = 0.1-0.7.	43	0	51.2%	±2.4%	MBD = -23.1% RMSD = 41.1%
Longo et al. [52] 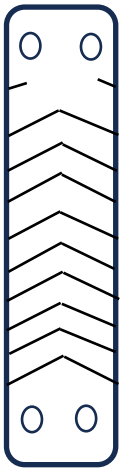	R1234ze(Z) and R1233zd(E), d_h = 4 mm, β = 65°, Z_P = 278 mm, A_P = 200 cm^2, q" = 12.15 kW/m^2, T_{sat} = 30-40°C,	41	0	48.8%	±14%	MBD = -37.9% RMSD = 60%

	G = 5.6-25.6 kg/m^2s.					

List of Figure Captions

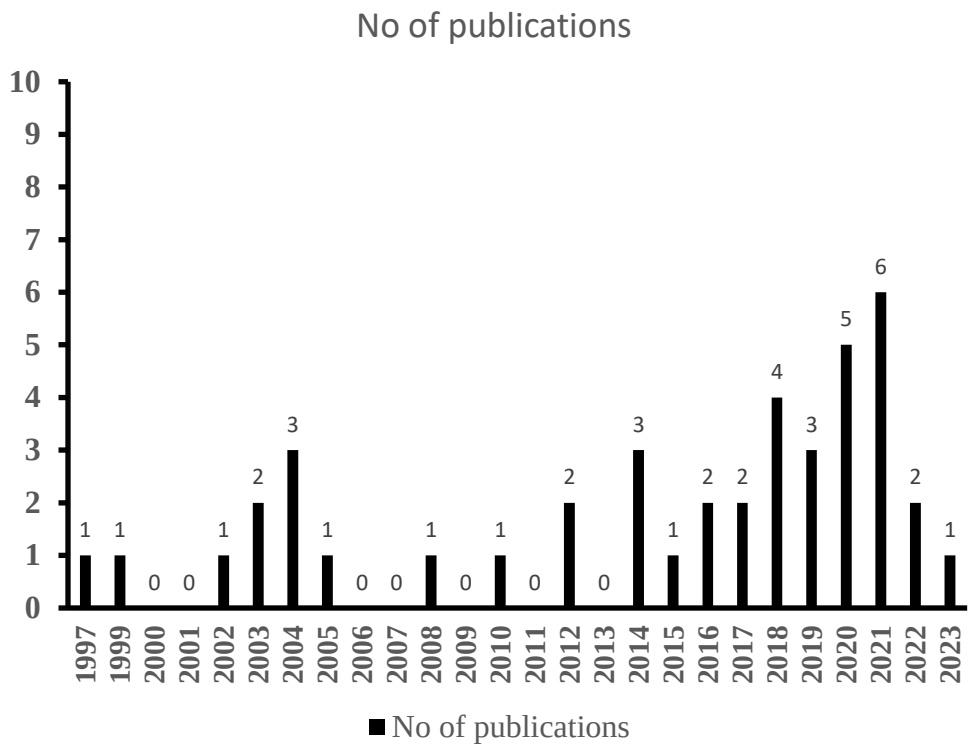

Figure 1 Publication record by year

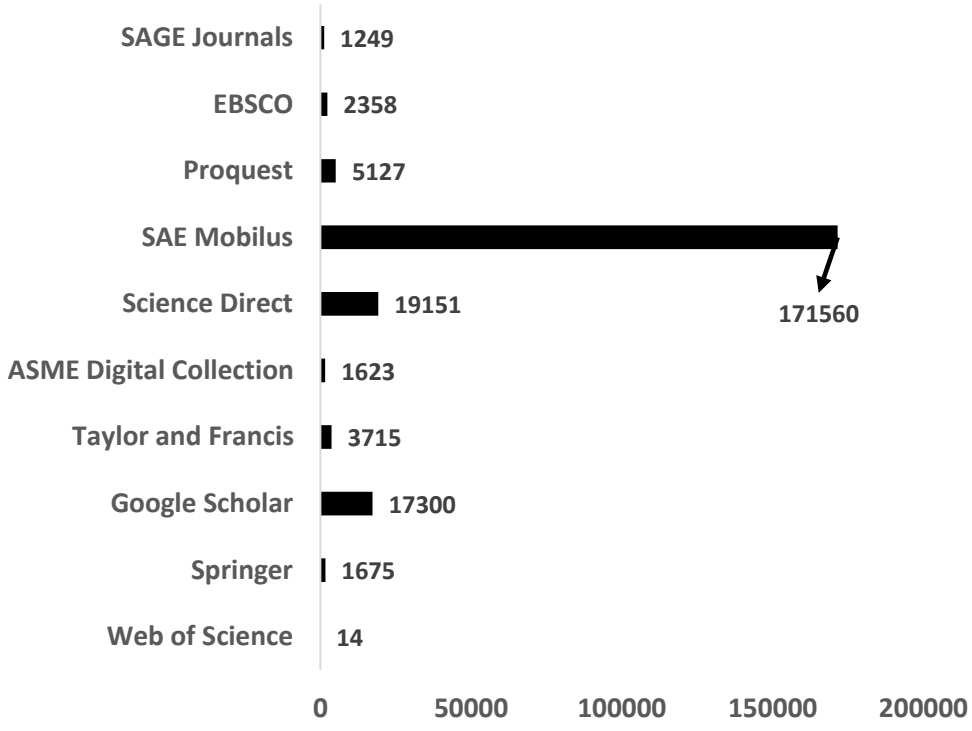

Figure 2 Database search by source and number of records

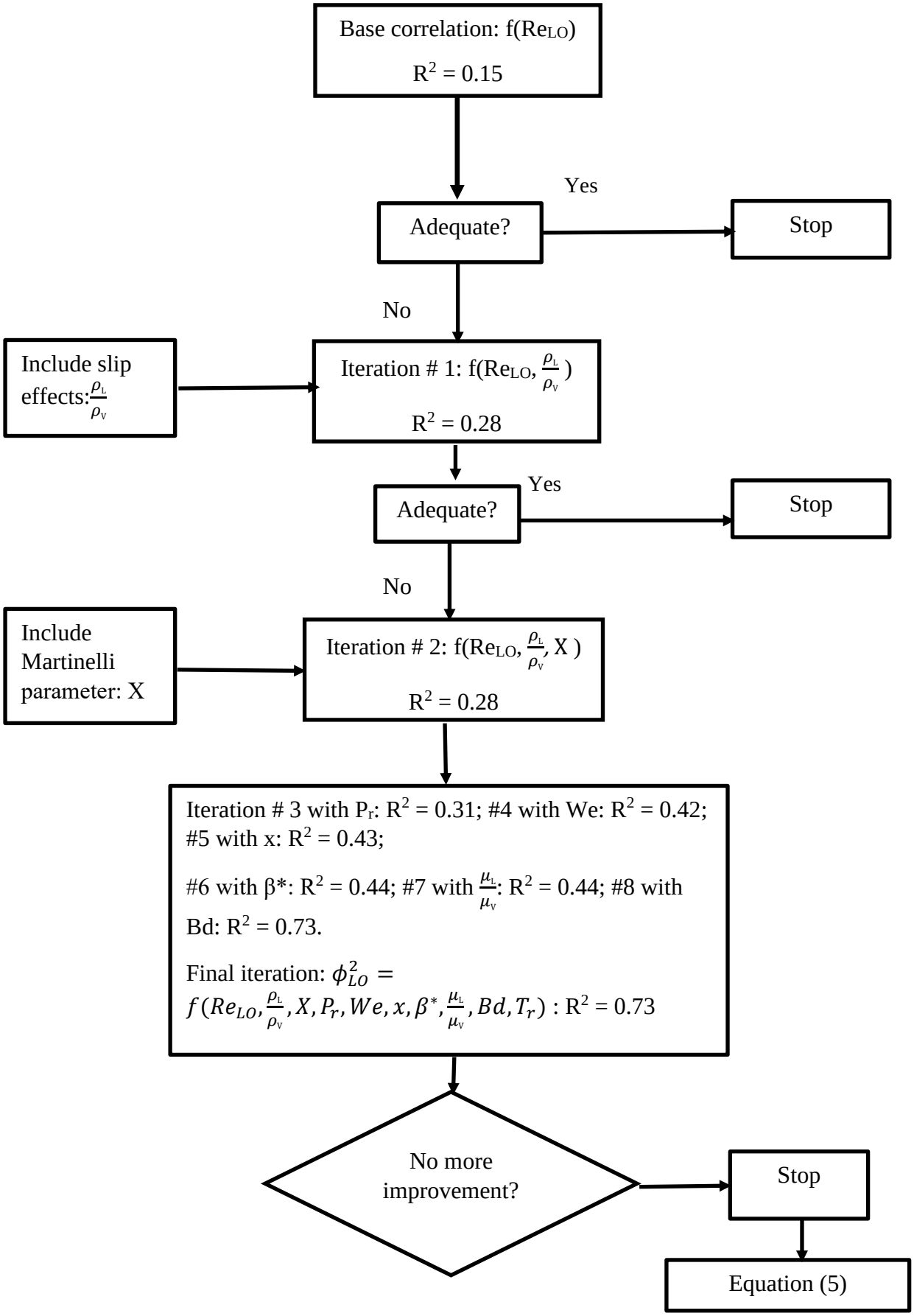

Figure 3 Iterative and decision-making chart for the condensation correlation Eq. (5)

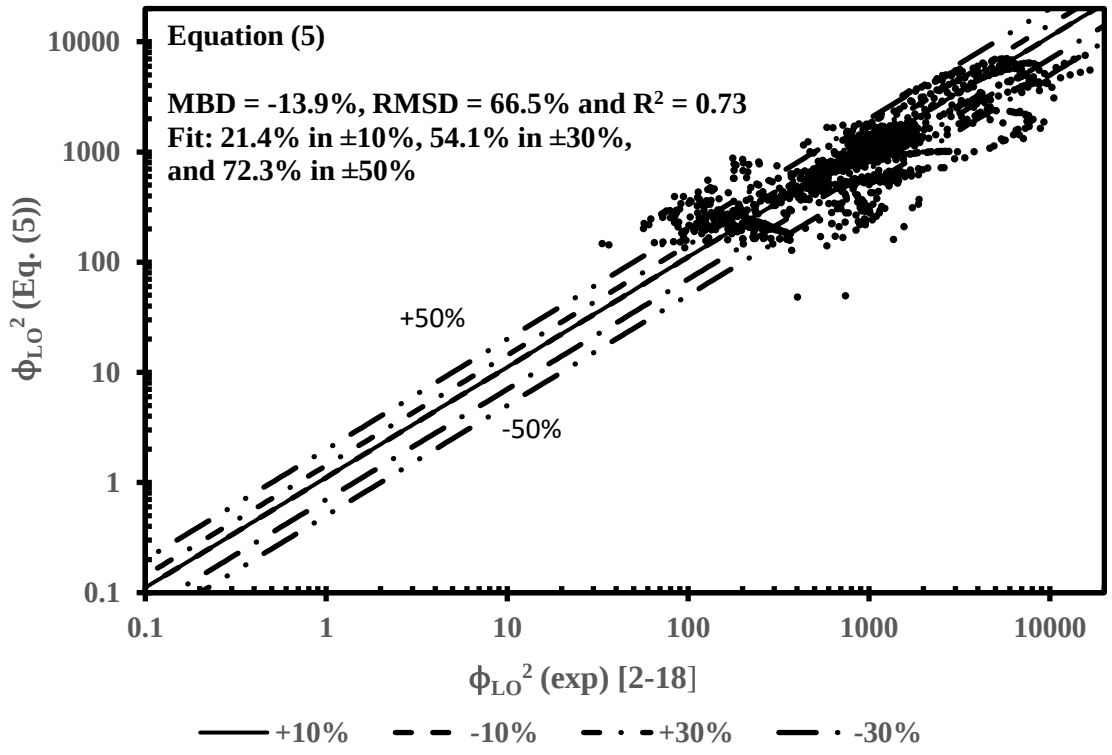

Figure 4 Predictive correlation (Eq. (5)) for the two-phase multiplier ϕ_{LO} in PHE condensers [2-18]

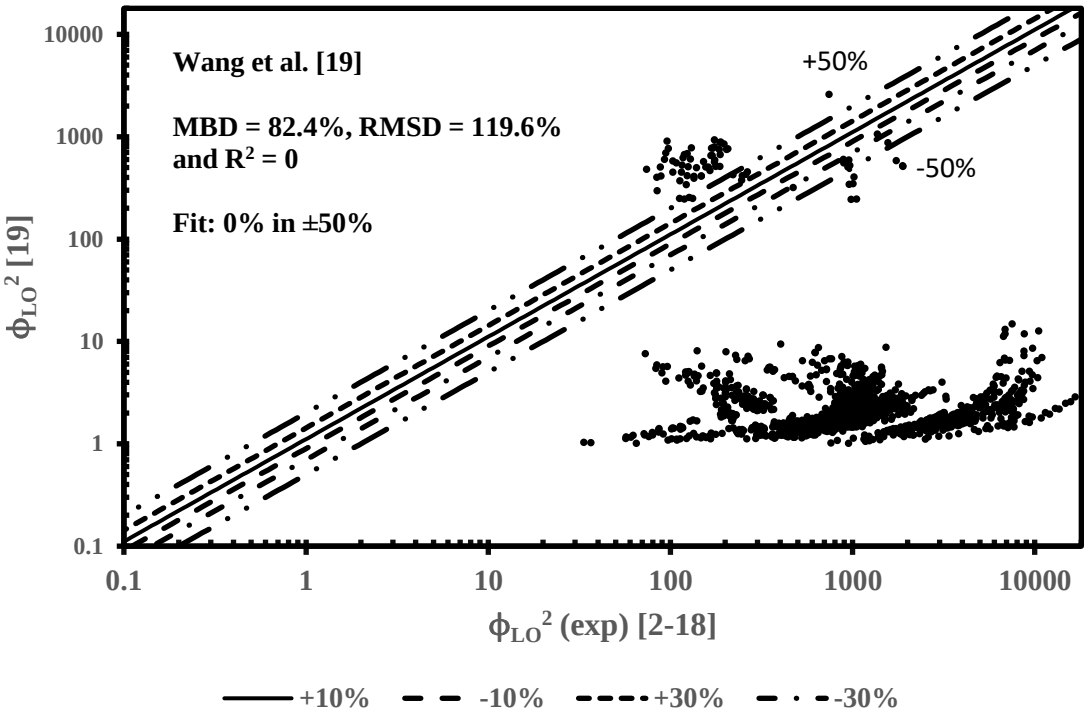

Figure 5 Comparison with the Wang et al. [19] correlation

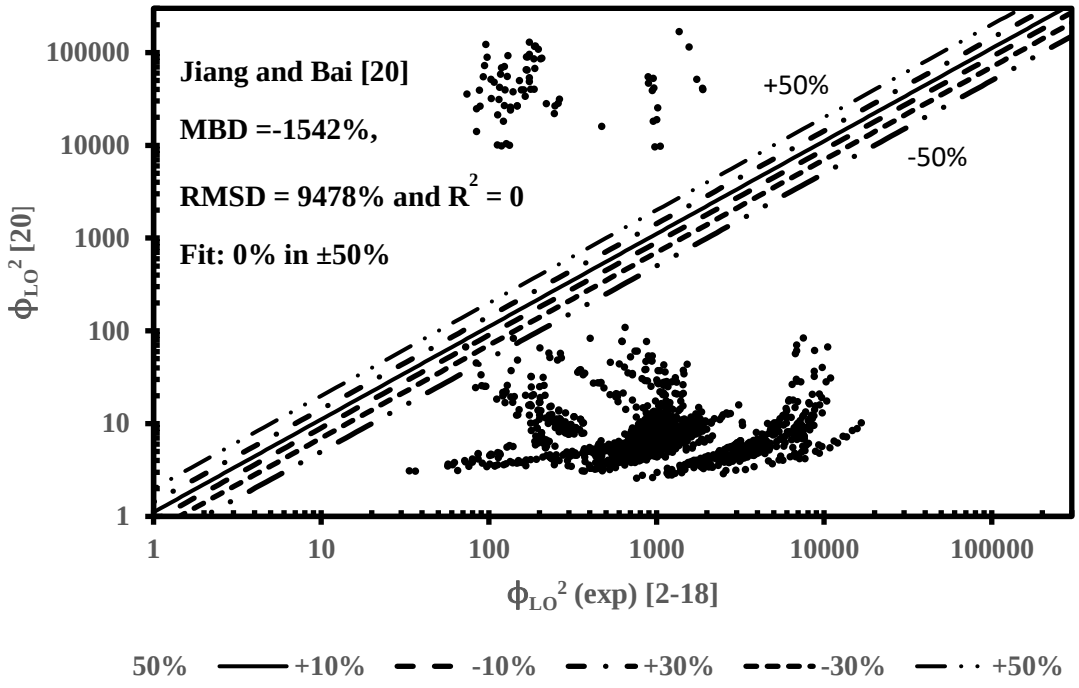

Figure 6 Comparison with the Jiang and Bai [20] correlation

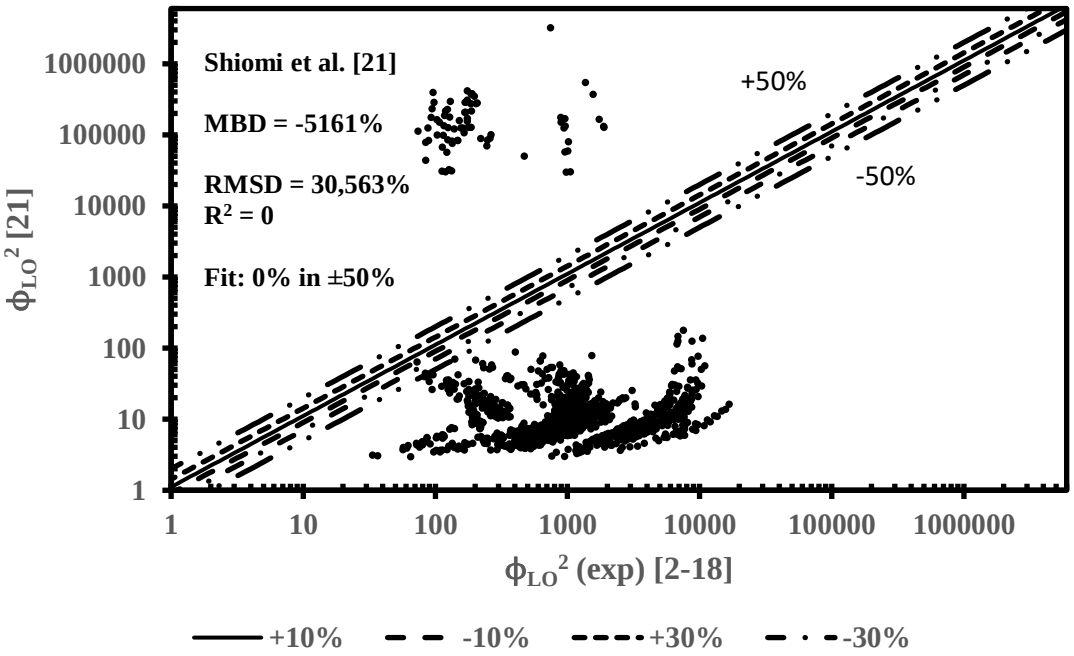

Figure 7 Comparison with the Shiomi et al. [21] correlation

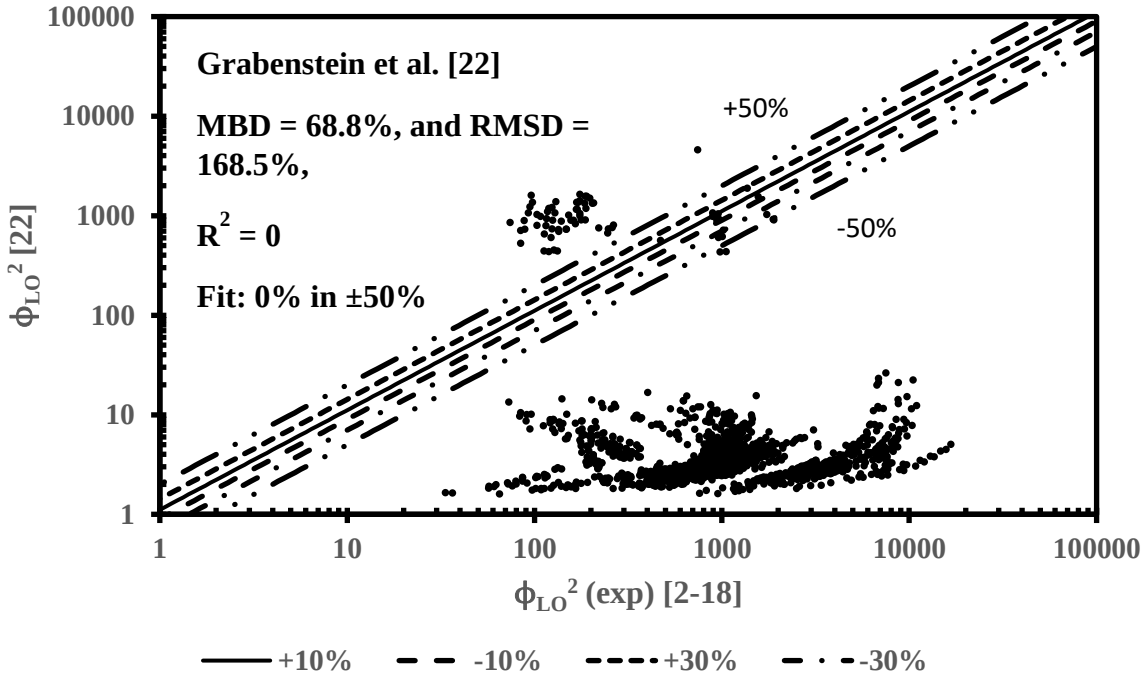

Figure 8 Comparison with the Grabenstein et al. [22] correlation

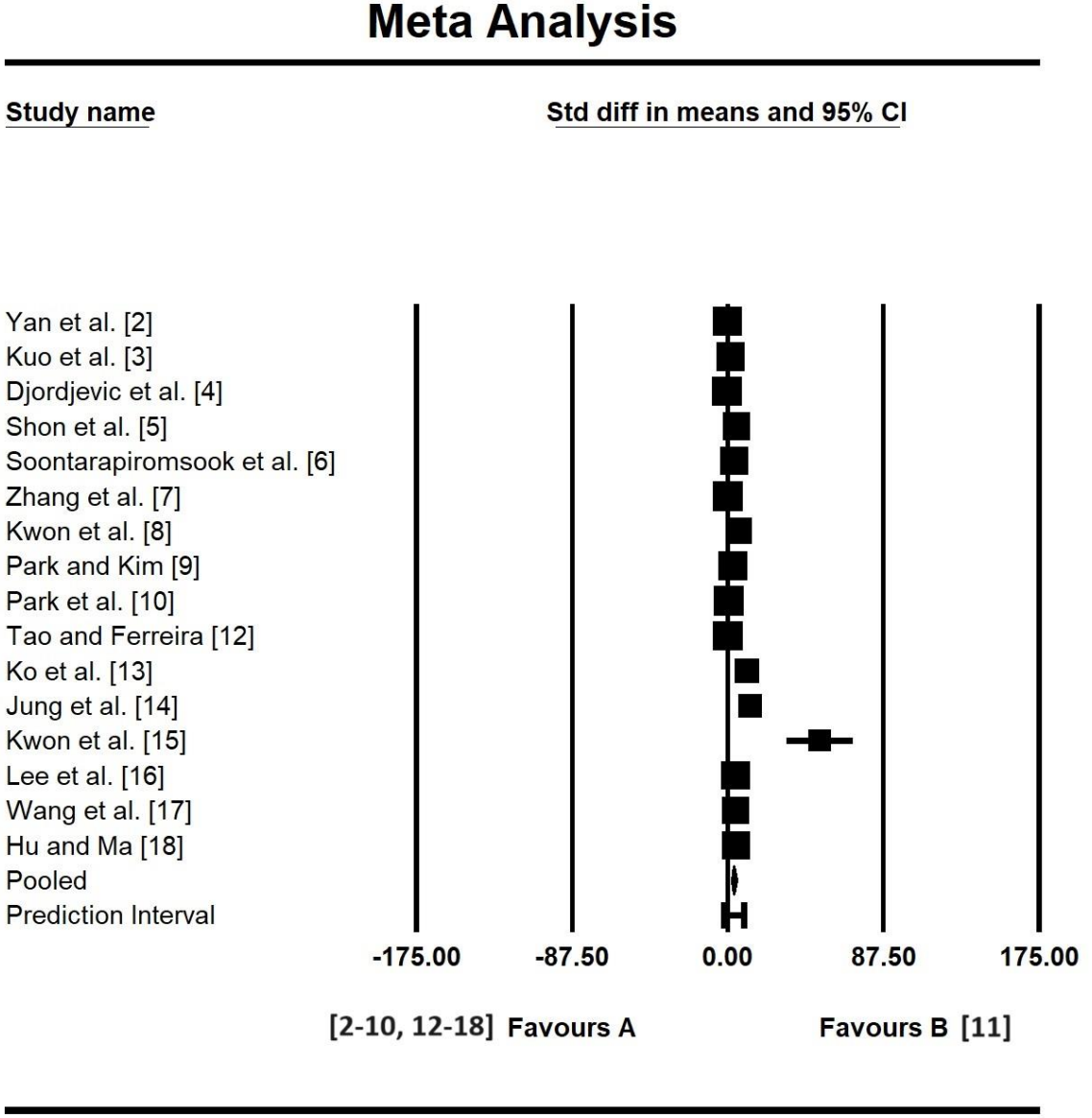

Figure 9 Meta-analysis of the two-phase multiplier ϕ_{LO} computed from the condensation pressure drop data [2-18]

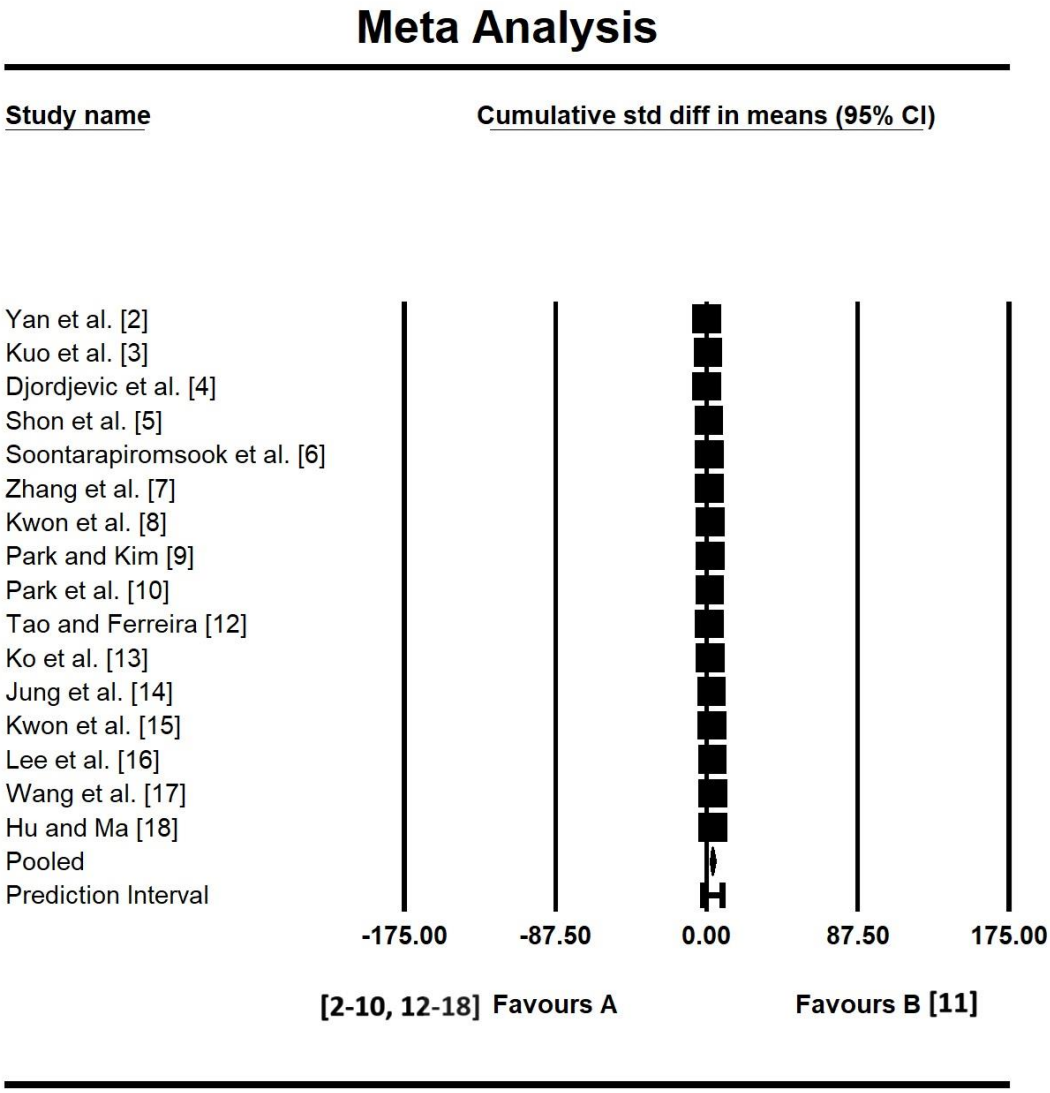

Figure 10 Cumulative meta-analysis of the two-phase multiplier ϕ_{LO} computed from the condensation pressure drop data [2-18]

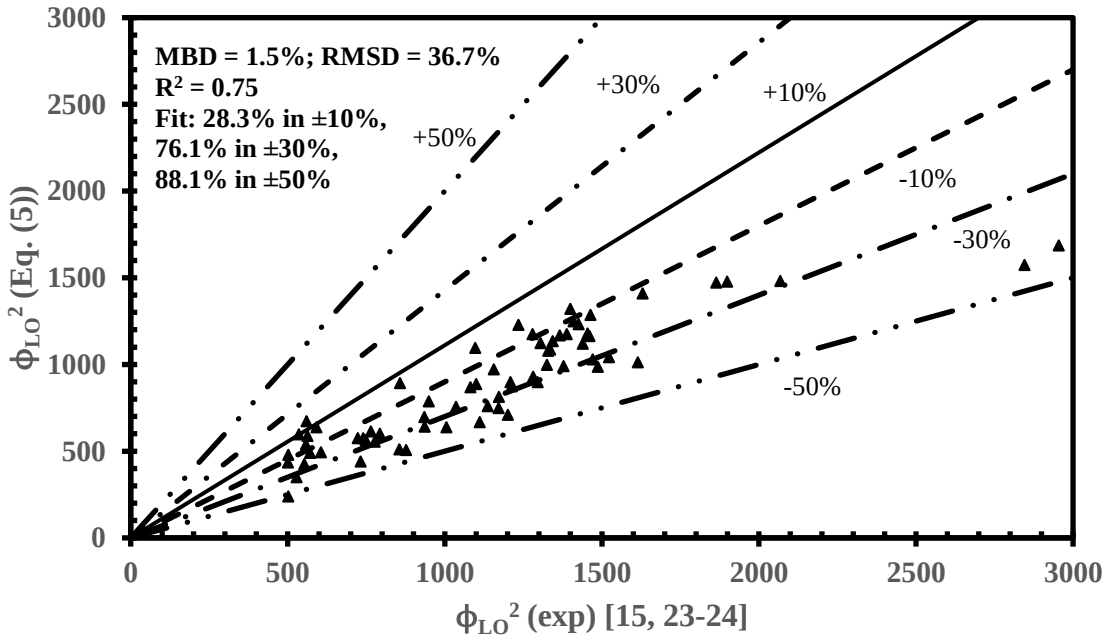

Figure 11 Evaluation of the condensation two-phase multiplier ϕ_{LO} correlation (Eq. (5)) with independent data [15, 23-24]

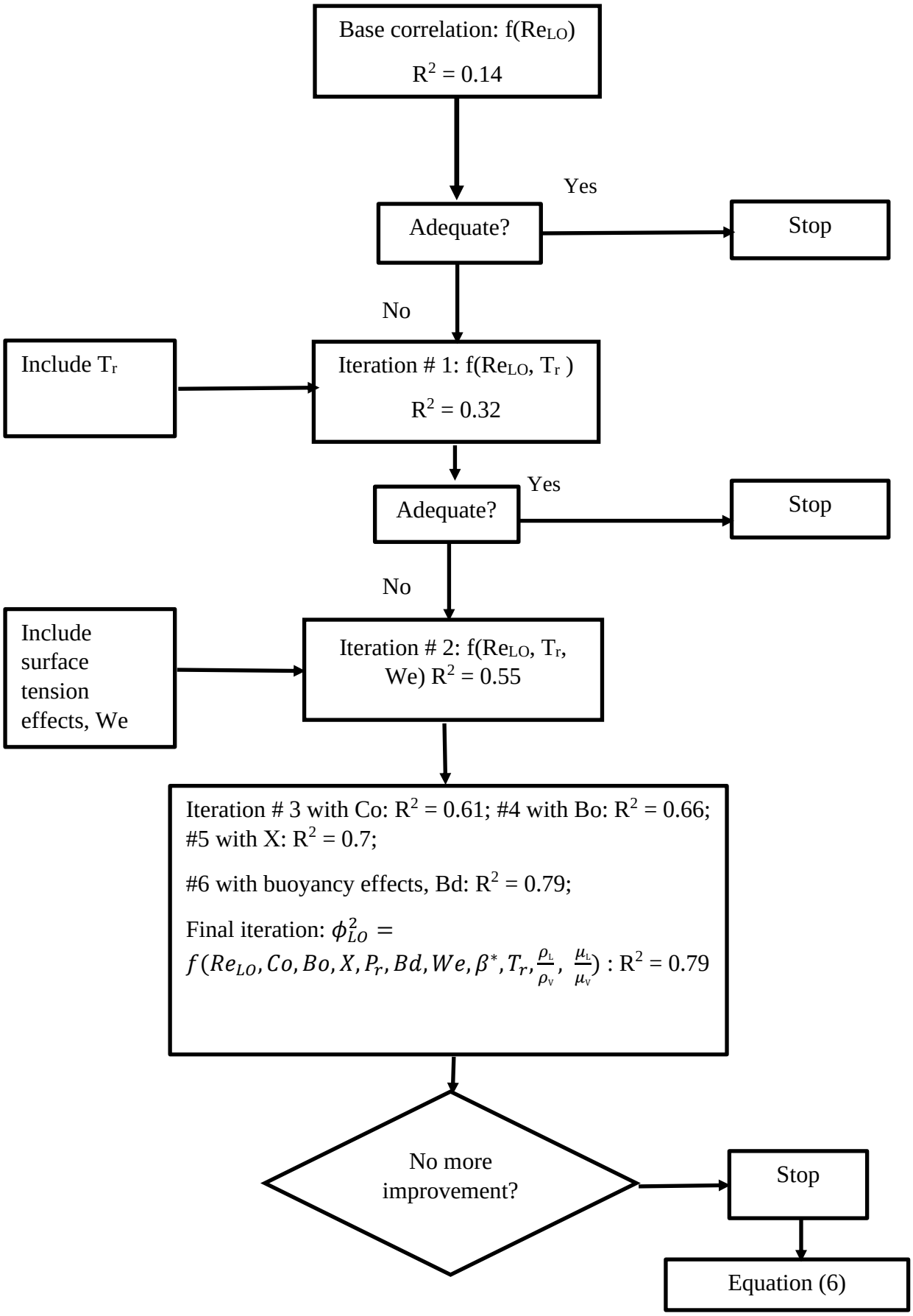

Figure 12 Iterative and decision-making chart for the evaporation correlation (Eq. (6))

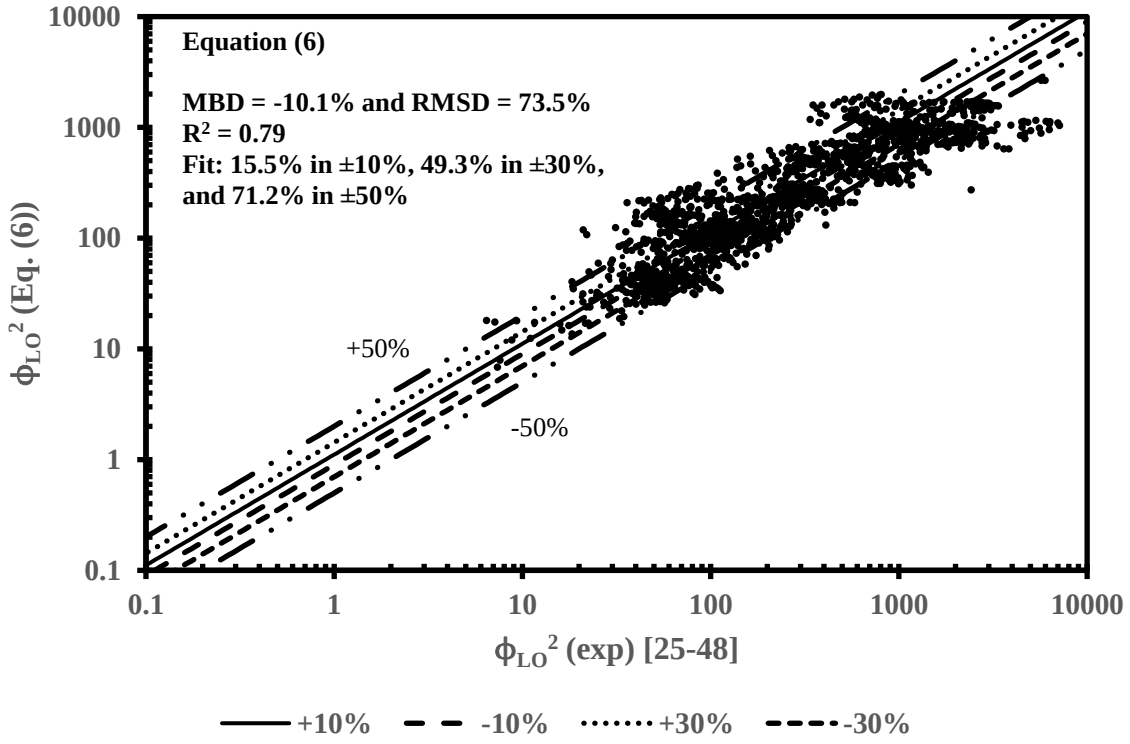

Figure 13 Empirical model (Eq. (6)) for the two-phase multiplier ϕ_{LO} in PHE evaporators [25-48]

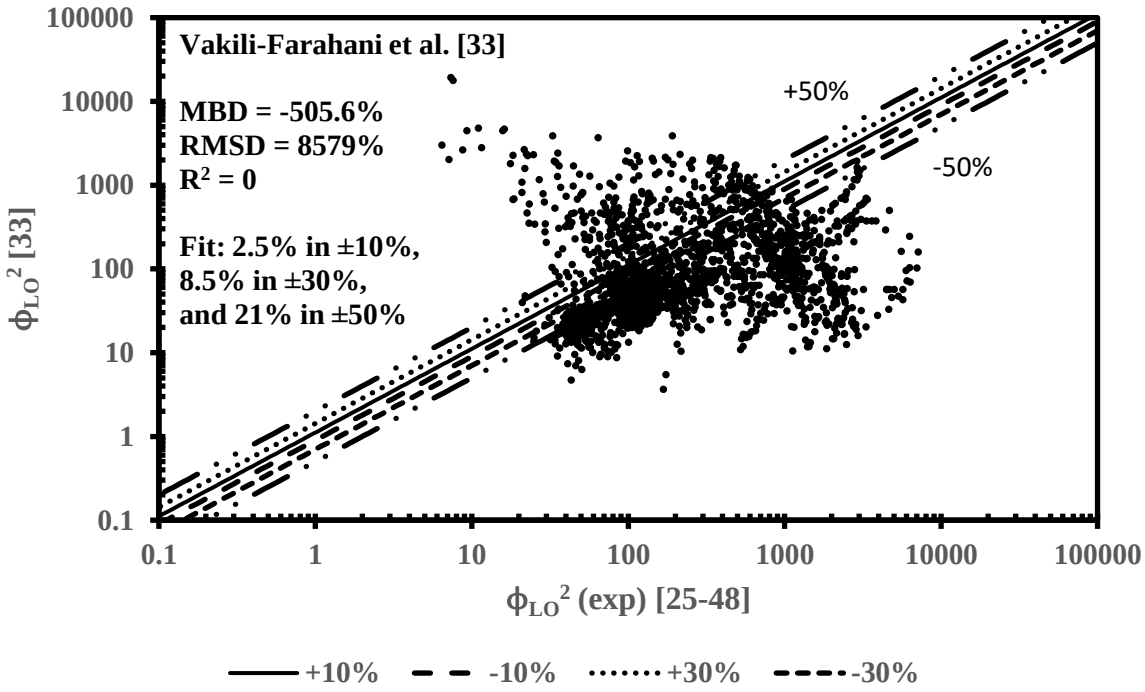

Figure 14 Comparison with the Vakili-Farahani et al. [33] correlation

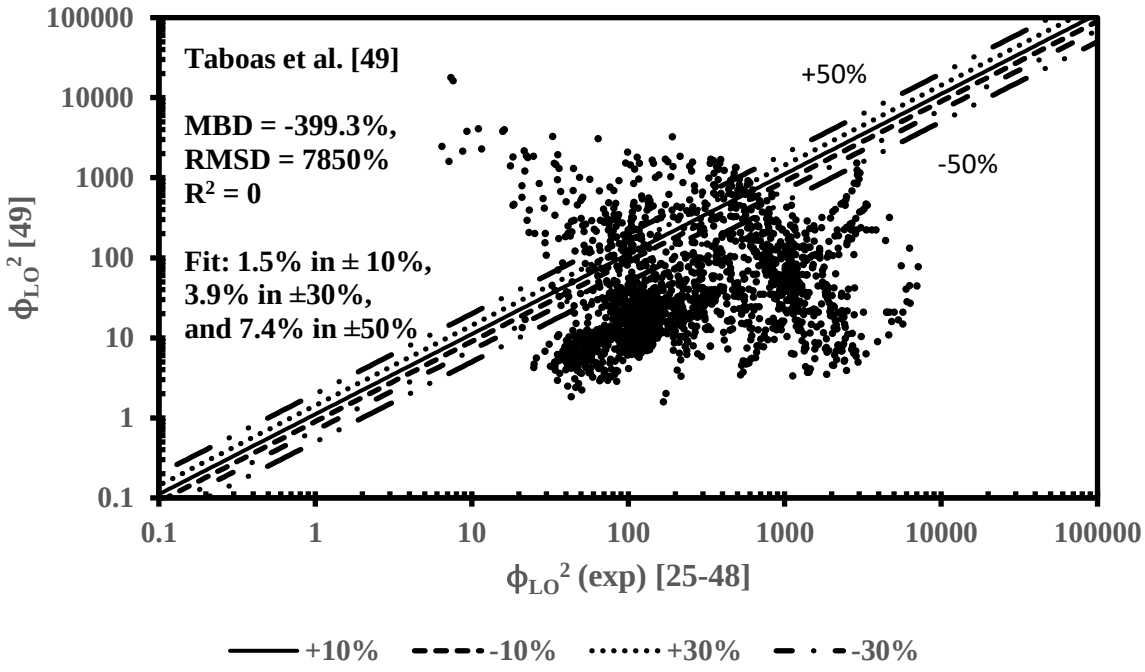

Figure 15 Comparison with the Taboas et al. [49] correlation

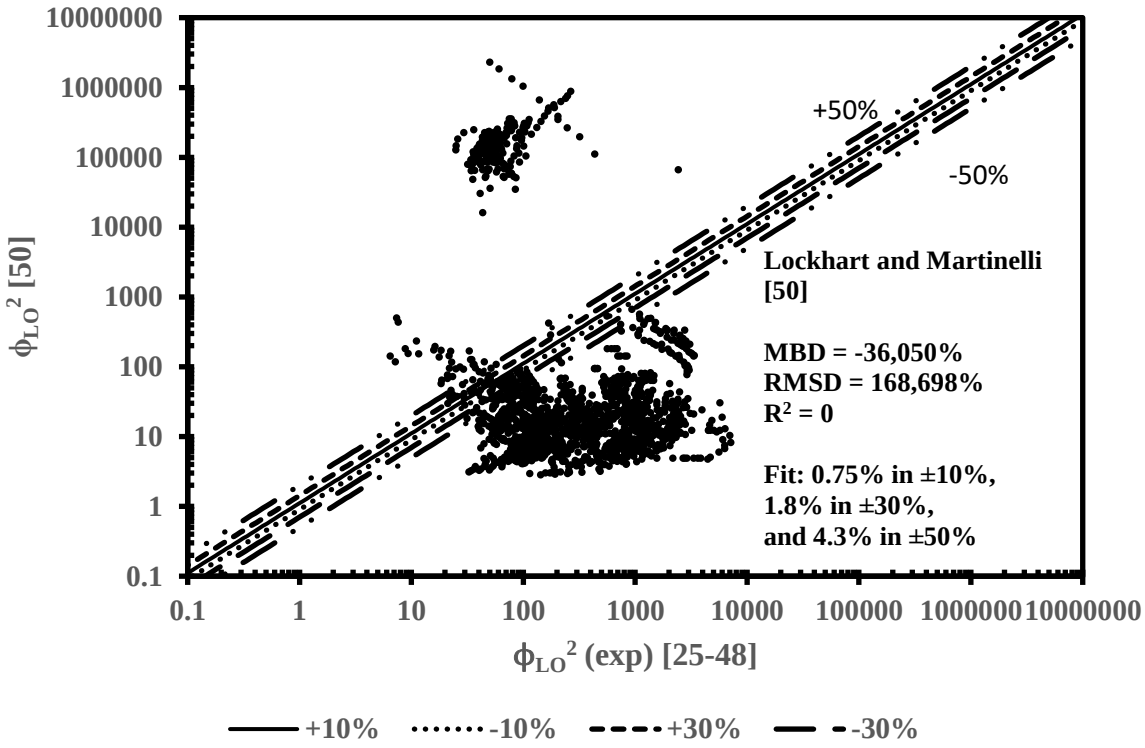

Figure 16 Comparison with the Lockhart and Martinelli [50] correlation

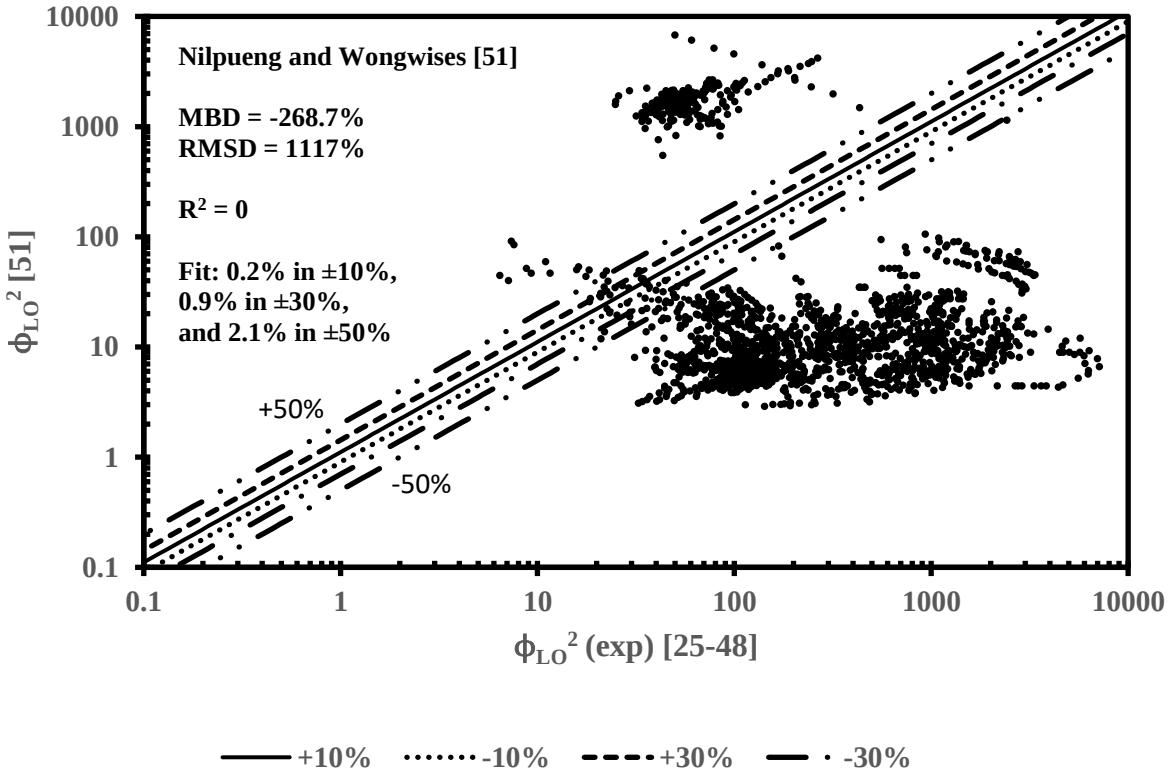

Figure 17 Comparison with the Nilpueng and Wongwises [51] correlation

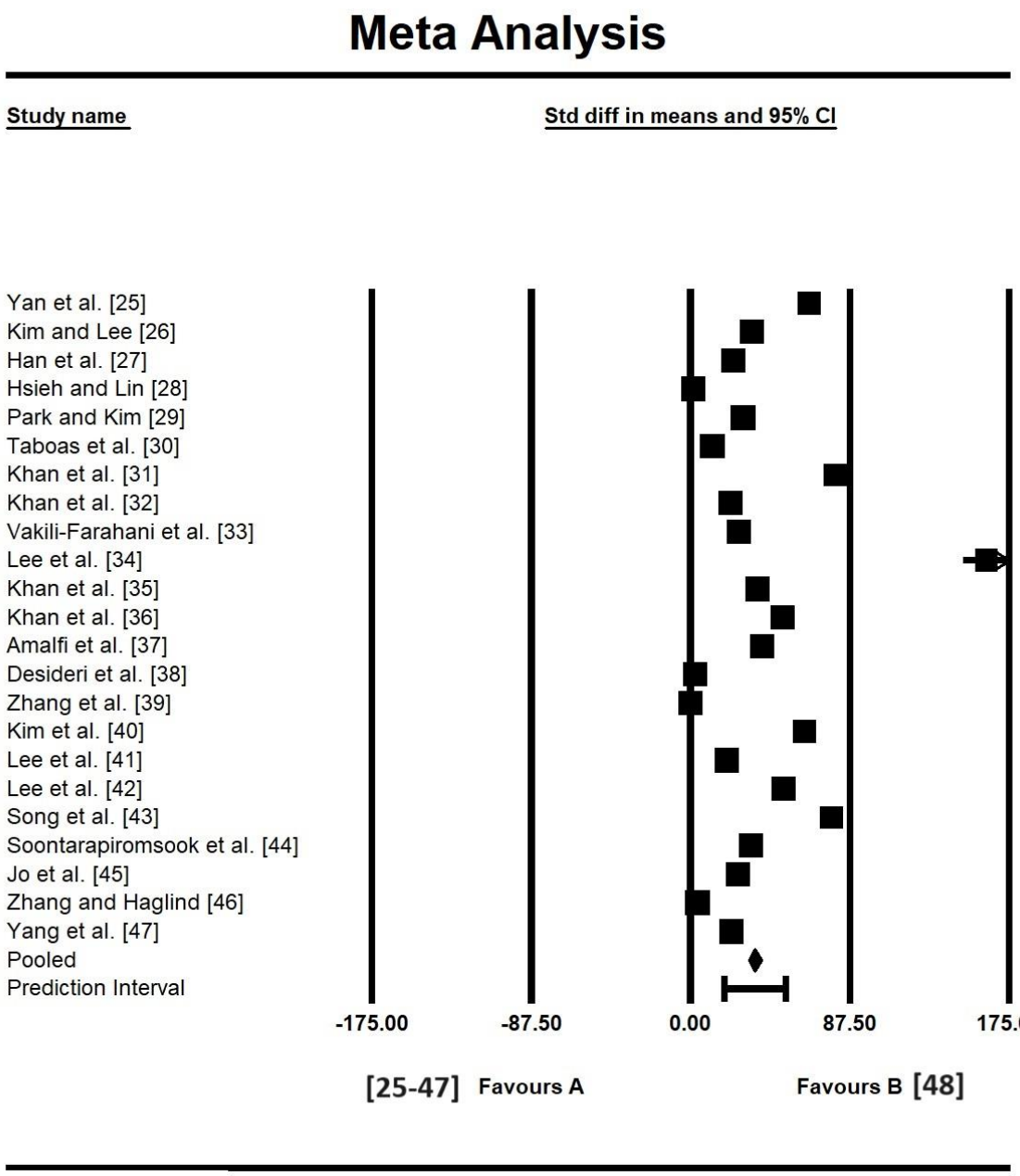

Figure 18 Meta-analysis of the two-phase multipliers ϕ_{LO} computed from the evaporation data in PHEs [25-48]

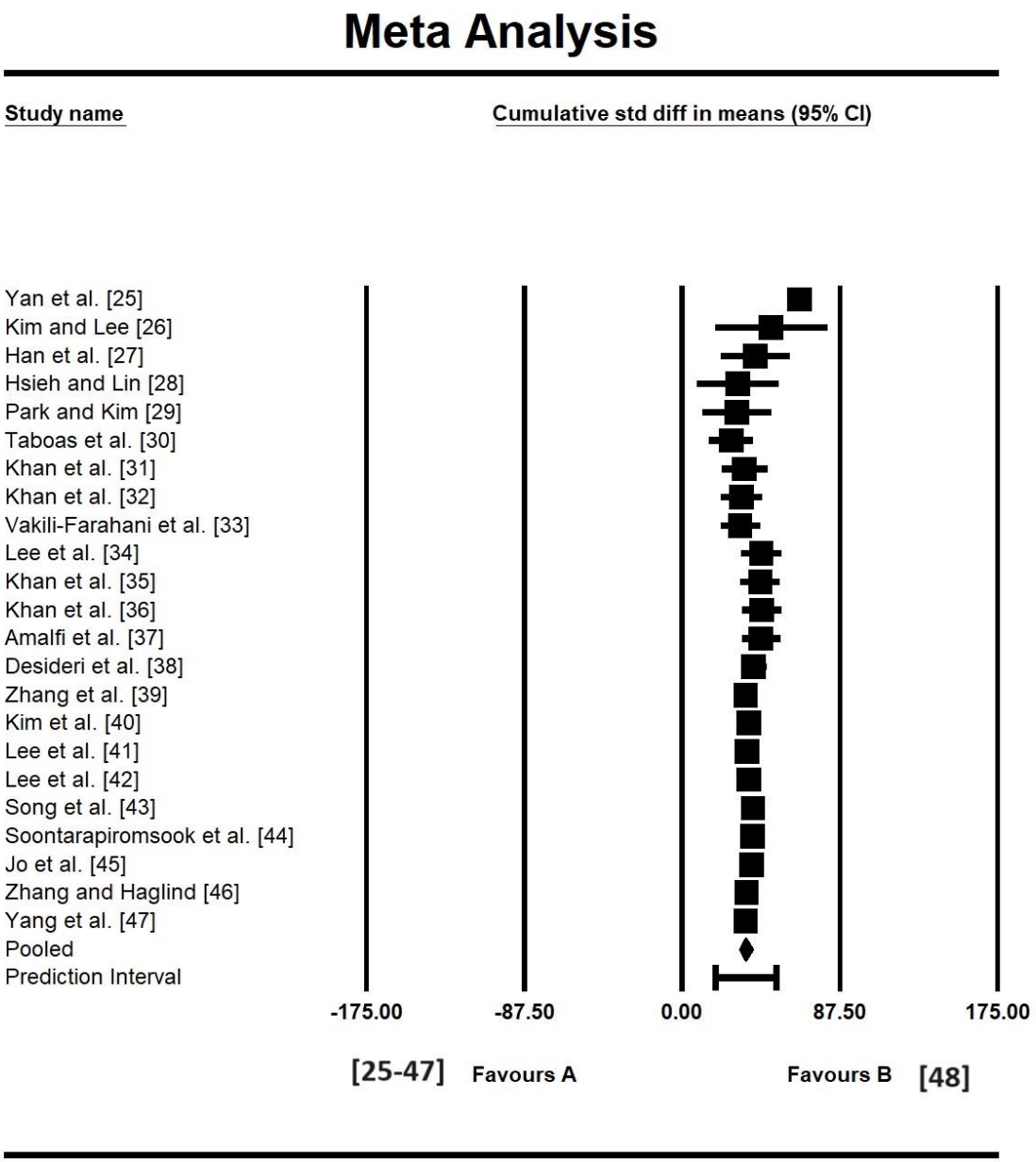

Figure 19 Cumulative meta-analysis of the two-phase multipliers ϕ_{LO} computed from the evaporation pressure drop data [25-48]

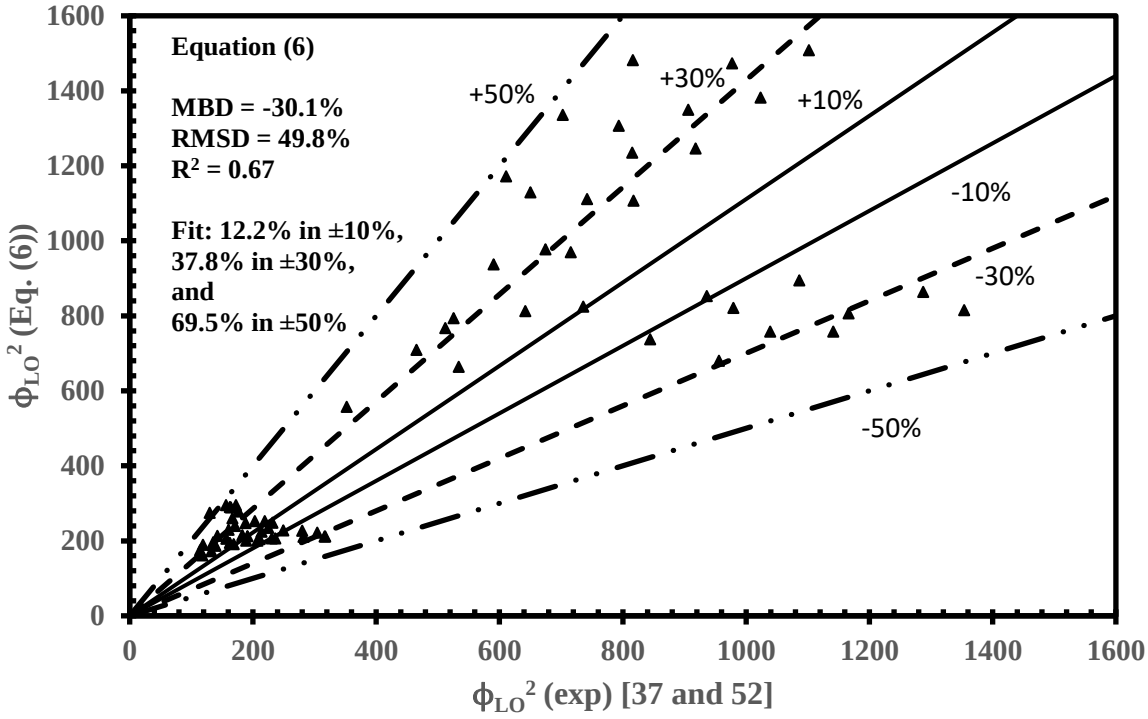

Figure 20 Validation of Eq. (6) with evaporation pressure drop data [37, 52]

Notes on Contributors

Yagnavalkya Mukkamala. Professor Mukkamala received his Ph.D. in Mechanical Engineering from Vellore Institute of Technology in 2008 and his M.S. in Mechanical Engineering from Virginia Polytechnic Institute and State University in 1993. He has published over nineteen articles in various peer-reviewed journals and peer-reviewed conference articles. He has completed several funded projects as a principal investigator for the Government of India and numerous as a student investigator for the US Department of Energy and NASA. He has been cited over two hundred and seventy times and has an h-index of over eight. His research interests include enhanced heat transfer, the design of enhanced heat exchangers, and automotive aerodynamics.

Professor Jaco Dirker is a professor of mechanical engineering at the University of Pretoria. He received his Ph.D. from Rand Afrikaans University (University of Johannesburg) in 2004. He has published over 44 peer-reviewed journals and 44 peer-reviewed conference articles. He has completed over five research projects, with the most recent project being funded by the Royal Society of the United Kingdom for over R 9 million (South African Rand). He is a clean energy and enhanced heat transfer specialist and has supervised several doctoral theses and post-doctoral scholars. He is a registered professional engineer at the Engineering Council of South Africa.